

Complexity of Classical Acceleration for ℓ_1 -Regularized PageRank

Kimon Fountoulakis*

University of Waterloo, Canada

kimon.fountoulakis@uwaterloo.ca

David Martínez-Rubio*

IMDEA Software Institute, Madrid, Spain

david.martinezrubio@imdea.org

February 25, 2026

Abstract

We study the degree-weighted work required to compute ℓ_1 -regularized PageRank using the standard one-gradient-per-iteration accelerated proximal-gradient method (FISTA). For non-accelerated local methods, the best known worst-case work scales as $\tilde{O}((\alpha\rho)^{-1})$, where α is the teleportation parameter and ρ is the ℓ_1 -regularization parameter. A natural question is whether FISTA can improve the dependence on α from $1/\alpha$ to $1/\sqrt{\alpha}$ while preserving the $1/\rho$ locality scaling. The challenge is that acceleration can break locality by transiently activating nodes that are zero at optimality, thereby increasing the cost of gradient evaluations. We analyze FISTA on a slightly over-regularized objective and show that, under a checkable confinement condition, all spurious activations remain inside a boundary set \mathcal{B} . This yields a bound consisting of an accelerated $(\rho\sqrt{\alpha})^{-1} \log(\alpha/\varepsilon)$ term plus a boundary overhead $\sqrt{\text{vol}(\mathcal{B})}/(\rho\alpha^{3/2})$. We provide graph-structural conditions that imply such confinement. Experiments on synthetic and real graphs show the resulting speedup and slowdown regimes under the degree-weighted work model.

1 Introduction

Personalized PageRank (PPR) is a diffusion primitive for exploring large graphs from a seed: starting from a node or distribution s , the diffusion returns a nonnegative score vector that concentrates near s and is widely used for local graph clustering and ranking [ACL06; Gle15]. A central algorithmic requirement in this setting is *locality*: the running time should scale with the size of the region around the target cluster, rather than with the total number of nodes or edges in the ambient graph.

A useful tool to obtain locality is adding ℓ_1 regularization, which induces sparsity at the solution. In the ℓ_1 -regularized PageRank formulation [GM14; FRS+19], one solves a strongly convex objective whose minimizer is sparse and nonnegative¹. Concretely, for teleportation parameter $\alpha \in (0, 1]$ and sparsity parameter $\rho > 0$, we consider problems of the form

$$\min_{x \in \mathbb{R}^n} \underbrace{\frac{1}{2} x^\top Q x - \alpha \langle D^{-1/2} s, x \rangle}_{\text{smooth PageRank quadratic}} + \underbrace{\alpha \rho \|D^{1/2} x\|_1}_{\ell_1 \text{ sparsity penalty}},$$

where D is the degree matrix and Q is a symmetric, scaled and shifted, Laplacian matrix, see Section 3. Let x^* denote the unique minimizer and let $S^* := \text{supp}(x^*)$ be its support.

For the above problem, the primitives of first-order methods can be implemented locally: if an iterate is supported on a set S , evaluating its gradient and performing a proximal gradient step only requires accessing edges incident to S . This motivates the degree-weighted work model [FRS+19], in which we charge one unit of work per neighbor access. Thus scanning the neighborhood of a vertex i costs d_i work, and the cost of a set S of non-zero nodes is $\text{vol}(S) := \sum_{i \in S} d_i$. The total work of an algorithm is the cumulative number of neighbor accesses with repetition performed over its execution.

Motivation. Accelerated first-order methods are worst-case optimal in gradient evaluations for smooth convex problems [Nes04; BT09], but for our objective, the cost per gradient depends on which nodes are active. Thus, sparsity governs the total work: ISTA is provably local, activating only the optimal support S^* [FRS+19], whereas FISTA

*Equal contribution.

¹This is a trivial corollary of [FRS+19], obtained by observing that the proximal-gradient iterates are nondecreasing when starting from zero.

forms extrapolated points y_k that can transiently create nonzeros outside S^* . Even a few such spurious activations can dramatically increase work (e.g., by touching high-degree nodes), so faster convergence in iterations does not imply less total work. We quantify this tradeoff and validate it empirically.

Our approach. We analyze FISTA under a degree-weighted work model that separates the work spent on the optimal support S^* and the cumulative work spent on transient coordinates outside that set. We bound the latter using two key ideas: (A) bounding transient activations from coordinates with a large complementary gap at x^* from the KKT conditions and (B) bounding the number of coordinates with small complementary gaps, by arguing that they belong to the support of an already sparse, slightly less regularized solution.

Total work bound and sufficient conditions. Under a verifiable confinement condition ensuring that all spurious activations remain within a boundary set \mathcal{B} , we obtain a work bound of the form

$$\tilde{O} \left(\frac{1}{\rho\sqrt{\alpha}} \log \left(\frac{\alpha}{\varepsilon} \right) + \frac{\sqrt{\text{vol}(\mathcal{B})}}{\rho\alpha^{3/2}} \right).$$

The first term is the accelerated cost of converging to the optimal support; the second term is an explicit overhead capturing the cumulative cost for exploring spurious nodes. We also give graph-structural sufficient conditions: a no-percolation criterion that makes the confinement hypothesis explicit and checkable. When this criterion holds with the target optimal support S^* as the core set, it guarantees that momentum-induced activations cannot percolate arbitrarily far into the graph: for all iterations k , the iterates remain supported in $S^* \cup \partial S^*$. In particular, any activation outside S^* is confined to the vertex boundary $\mathcal{B} := \partial S^*$, so the locality overhead in our work bound is governed by the boundary volume $\text{vol}(\mathcal{B}) = \text{vol}(\partial S^*)$. This makes the second term directly interpretable as the cost of probing only the immediate neighborhood of the target support.

Experiments. Finally, experiments on synthetic instances and SNAP [LK14] graphs corroborate the predicted speedup/slowdown regimes under degree-weighted work: acceleration helps when boundary exploration is limited, and it can hurt when transient boundary activations dominate.

Contributions. Our main contributions can be summarized as follows.

- *From KKT slack to cumulative spurious work.* We prove that any activation of an inactive coordinate (that is, which is zero at the solution) implies a quantitative “jump” in per-iteration work, controlled by its KKT slack (complementarity gap). We combine this fact with FISTA’s geometric contraction to bound the total degree-weighted work spent on such spurious activations.
- *Avoid tiny margins via over-regularization.* The smallest KKT slack can be arbitrarily small, see Section C, which would make our work bound meaningless. To fix this, we analyze a slightly more regularized problem and use regularization-path monotonicity [HFM21] to treat “nearly active” nodes as part of the true solution, and charge extra work only to nodes that remain clearly inactive.
- *A worst-case work bound for classic FISTA.* Under a boundary confinement condition (spurious activations stay within a boundary set \mathcal{B}), we obtain an explicit work bound with an accelerated term $\tilde{O}((\rho\sqrt{\alpha})^{-1} \log(\alpha/\varepsilon))$ plus a boundary overhead quantified by $\text{vol}(\mathcal{B})$ (cf. Theorem 4.3).
- *Graph-structural confinement guarantees and degree-based non-activation.* We give a sufficient no-percolation condition for boundary confinement, and we characterize (in Section B) when high-degree inactive nodes provably never activate under over-regularization.

2 Related work

Personalized PageRank (PPR) and related diffusion vectors are widely used primitives for ranking and network analysis beyond web search (see, e.g., the survey [Gle15]). A foundational locality result is due to Andersen, Chung, and Lang [ACL06], who introduced the Approximate Personalized PageRank (APPR) “push” procedure and showed that one can compute an ε -approximate PPR vector in time $\tilde{O}(1/(\alpha\varepsilon))$ independent of the graph size. This establishes that diffusion solutions can be computed locally and used for local graph partitioning.

Variational formulations and worst-case locality for non-accelerated methods. The variational perspective of Gleich and Mahoney [GM14] and Fountoulakis et al. [FRS+19] shows that a standard local clustering guarantee (in the spirit of APPR) can be obtained by solving an ℓ_1 -regularized PageRank objective. Fountoulakis et al. [FRS+19] show

that proximal-gradient/ISTA iterations can be implemented locally on undirected graphs, with total work $\tilde{O}((\alpha\rho)^{-1})$ to reach a prescribed accuracy, where ρ is the regularization parameter. This gives a worst-case, graph-size-independent work bound for non-accelerated optimization. What is missing is an analogous worst-case bound for accelerated proximal-gradient methods. A related line studies statistical and regularization-path properties of local diffusion objectives. For instance, Ha, Fountoulakis, and Mahoney [HFM21] develop statistical guarantees for local graph clustering and analyze properties of the ℓ_1 -regularized PageRank solution path, which is a structural tool (e.g., monotonicity along the regularization path) that we leverage when reasoning about over-regularization in our paper.

The COLT’22 open problem on acceleration and its solutions/attempts. Fountoulakis and Yang [FY22] posed the COLT’22 open problem of whether one can obtain a provable accelerated algorithm for ℓ_1 -regularized PageRank with work $\tilde{O}((\rho\sqrt{\alpha})^{-1})$, improving the α -dependence by a factor of $1/\sqrt{\alpha}$ over ISTA while preserving locality. They emphasized that existing ISTA analyses do not cover acceleration and that it was unclear whether worst-case work might even degrade under acceleration. The first affirmative solution is due to Martínez-Rubio, Wirth, and Pokutta [MWP23], who design accelerated algorithms that retain sparse updates. Their method *ASPR* uses an expanding-subspace (outer-inner) scheme: it grows a set of “good” coordinates and runs an accelerated projected gradient subroutine on the restricted feasible set. This yields a worst-case bound of $O(|S^*|\widetilde{\text{vol}}(S^*)\alpha^{-1/2}\log(1/\varepsilon) + |S^*|\text{vol}(S^*))$, where S^* is the support of the optimal solution and $\widetilde{\text{vol}}(S^*)$ is the number of edges of the subgraph formed only by nodes in S^* . Compared to $O(\text{vol}(S^*)\alpha^{-1}\log(1/\varepsilon)) = \tilde{O}(1/(\rho\alpha))$ of ISTA, the solution improves the α -dependence with a different sparsity dependence than ISTA. In this work, we provide a support-sensitive, degree-weighted work analysis of the classic *one-gradient-per-iteration* FISTA method. Our contribution is algorithmically orthogonal, and the bound establishes a new trade-off under checkable conditions. Zhou et al. [ZSB+24] study locality for accelerated linear-system solvers via a “locally evolving set process” and obtain an accelerated guarantee under an additional run-dependent residual-reduction assumption, which they note is empirically reasonable but not yet theoretically justified. In contrast, our bounds for standard FISTA are checkable, and we quantify when classical acceleration reduces total degree-weighted work and when boundary exploration can dominate.

Support identification, strict complementarity. Our complementarity-gap viewpoint connects to the constraint-identification literature: under strict-complementarity-type conditions, proximal and proximal-gradient methods identify the optimal support in finitely many iterations [BM94; NSH19; SJN+19], and acceleration can delay identification via oscillations [BI20] (see also related strict-complementarity analyses for Frank-Wolfe [Wol70; GM86; Gar20]). To the best of our knowledge, these identification results are iteration-complexity statements under unit-cost gradient/prox steps, and they do not quantify a locality-aware total work measure for accelerated methods.

3 Preliminaries and notation

We assume undirected and unweighted graphs, and we use $[n] := \{1, \dots, n\}$. $\|\cdot\|_2$ denotes the Euclidean norm and $\|\cdot\|_1$ denotes the ℓ_1 norm. For a set $S \subseteq [n]$ we write $|S|$ for its cardinality. If the indices in S represent node indices of a graph, we use $\text{vol}(S) := \sum_{i \in S} d_i$ for the graph volume, where d_i is the number of neighbors of node i , that is, its degree. We assume $d_i > 0$ for all vertices.

We say a differentiable function f is L -smooth if ∇f is L -Lipschitz with respect to $\|\cdot\|_2$, that is $\|\nabla f(x) - \nabla f(y)\|_2 \leq L\|x - y\|_2$. We denote by $\mu > 0$ the strong-convexity parameter of a strongly-convex function F with respect to $\|\cdot\|_2$. In such a case F has a unique minimizer x^* . For one such problem, define the optimal support and its complement as $S^* := \text{supp}(x^*)$ and $I^* := [n] \setminus S^*$.

The main objective that we consider in this work is the personalized PageRank quadratic objective, and its ℓ_1 regularized version. For a parameter $\alpha > 0$, called the teleportation parameter, and an initial distribution of nodes s (i.e., $\langle \mathbf{1}, s \rangle = 1, s \geq 0$), the unregularized PageRank objective is

$$f(x) := \frac{1}{2}\langle x, Qx \rangle - \alpha\langle D^{-1/2}s, x \rangle \text{ for } Q = \alpha I + \frac{1-\alpha}{2}\mathcal{L},$$

where $\mathcal{L} := I - D^{-1/2}AD^{-1/2}$ is the symmetric normalized Laplacian matrix, which is known to satisfy $0 \preceq \mathcal{L} \preceq 2I$ [BC14]. Thus, $\alpha I \preceq Q \preceq I$, which implies the objective is α -strongly convex and 1-smooth. We will assume the seed is a single node v , that is $s = e_v$. This is the case for clustering applications, where one seeks to find a cluster of nodes near v that have high intraconnectivity and low connectivity to the rest of the graph [ACL06; Gle15].

A common objective for obtaining sparse PageRank solutions is the ℓ_1 -Regularized Personalized PageRank problem (RPPR), which comes with the sparsity guarantee $\text{vol}(S^*) \leq 1/\rho$, cf. [FRS+19, Theorem 2], where $\rho > 0$ is a

regularization weight on the objective:

$$\min_{x \in \mathbb{R}^n} F_\rho(x) := \min_{x \in \mathbb{R}^n} f(x) + g(x) = \min_{x \in \mathbb{R}^n} f(x) + \alpha\rho \|D^{1/2}x\|_1. \quad (\text{RPPR})$$

where $g(x) := \alpha\rho \|D^{1/2}x\|_1$. This is the central problem we study in this work.

It is worth noticing some properties of (RPPR). The initial gap from $x_0 = 0$ is $\Delta_0 := F(0) - F(x^*) \leq \alpha/2$, cf. Lemma A.1, and so by strong convexity, the initial distance to x^* satisfies $\|0 - x^*\|_2 \leq \sqrt{2\Delta_0/\mu} \leq 1$. Finally, the minimizer $x^*(\rho)$ of F_ρ is coordinatewise nonnegative and the optimality conditions are, cf. [FRS+19]:

$$\nabla_i f(x^*(\rho)) \in \begin{cases} \{-\alpha\rho\sqrt{d_i}\}, & x_i^*(\rho) > 0, \\ [-\alpha\rho\sqrt{d_i}, 0], & x_i^*(\rho) = 0. \end{cases} \quad (1)$$

3.1 The FISTA Algorithm

We introduce here the classical accelerated proximal-gradient method (FISTA) [BT09] and the properties we use later. We present the method for a composite objective $F(x) := f(x) + g(x)$ where f is L -smooth and F is μ -strongly convex with respect to $\|\cdot\|_2$. For (RPPR), we have $L = 1$ and $\mu = \alpha$ (since $\alpha I \preceq Q \preceq I$), so the standard choice is step size $\eta = 1/L = 1$ and momentum parameter $\beta = \frac{\sqrt{L/\mu-1}}{\sqrt{L/\mu+1}} = \frac{1-\sqrt{\alpha}}{1+\sqrt{\alpha}}$. The iterates of the FISTA algorithm initialized with $x_{-1} = x_0 = 0$ are, for $k \geq 0$:

$$y_k = x_k + \beta(x_k - x_{k-1}), \quad x_{k+1} = \text{prox}_{\eta g}(y_k - \eta \nabla f(y_k)). \quad (\text{FISTA})$$

The proximal operator is defined as $\text{prox}_{\eta g}(x) := \arg \min_y \{\eta g(y) + \frac{1}{2}\|y - x\|_2^2\}$. For the RPPR regularizer $g(x) = \alpha\rho \|D^{1/2}x\|_1$ the prox is separable and yields:

$$x_{k+1,i} = \text{sign}(y_{k,i} - \eta \nabla_i f(y_k)) \max\{|y_{k,i} - \eta \nabla_i f(y_k)| - \eta\alpha\rho\sqrt{d_i}, 0\}. \quad (2)$$

Definition 3.1 We measure runtime via a degree-weighted work model. For an iterate pair (y_k, x_{k+1}) we define the per-iteration work as

$$\text{work}_k := \text{vol}(\text{supp}(y_k)) + \text{vol}(\text{supp}(x_{k+1})). \quad (3)$$

For ISTA, $y_k = x_k$; for FISTA, $y_k = x_k + \beta(x_k - x_{k-1})$. The total work to reach the stopping target is the sum of work_k over the iterations taken².

4 FISTA's work analysis in RPPR under ℓ_1 over-regularization

We analyze the work of (FISTA) on (RPPR). In this setting, fewer iterations do not automatically mean less work. Although FISTA improves the iteration complexity of ISTA, its extrapolated points y_k can transiently activate coordinates that are zero at the optimizer, increasing the cost of computing the gradient at each iteration. Our analysis splits the work into a core cost and a spurious-exploration overhead. We fix a core set S that we are willing to pay for at every iteration, and we charge any additional work to the spurious active sets outside S , namely $\tilde{A}_k := \text{supp}(x_{k+1}) \cap S^c$. We show that the additional work is inversely proportional to the minimum KKT margin. To avoid vacuous bounds when KKT margins are tiny, we choose $S = \text{supp}(x^*(\rho))$, while our target is $F_{2\rho}$. By the RPPR sparsity guarantee, this implies $\text{vol}(S) \leq 1/\rho$ (cf. Section 3). The remainder of the section bounds the cumulative overhead $\sum_k \text{vol}(\tilde{A}_k)$ via complementarity slacks, confinement condition, and FISTA's iteration complexity.

²Since each FISTA iteration computes a single gradient at y_k , one could alternatively take $\text{work}_k := \text{vol}(\text{supp}(y_k))$. Our definition (3) is a convenient symmetric upper bound (it also covers evaluations at x_{k+1} , e.g., for stopping diagnostics), and it matches the quantities controlled in our proofs up to an absolute constant.

4.1 Over-regularization

A direct locality analysis of accelerated proximal-gradient methods naturally runs into a margin issue. In the arguments that follow, spurious activations will be controlled by KKT slacks at the optimum. For RPPR, however, the smallest slack over inactive coordinates can be arbitrarily small (see Section C), so any bound that depends on the minimum slack would be vacuous. To obtain a work bound that remains meaningful, we will slightly over-regularize the objective, and we will relate the support of the solutions for $F_{2\rho}$ and F_ρ . For these two problems, we introduce the notation:

$$g_A(x) := \alpha\rho\|D^{1/2}x\|_1 \quad \text{and} \quad g_B(x) := 2\alpha\rho\|D^{1/2}x\|_1,$$

and the corresponding minimizers

$$x_A^* \in \arg \min_x (f(x) + g_A(x)), \quad x_B^* \in \arg \min_x (f(x) + g_B(x)),$$

with supports $S_A := \text{supp}(x_A^*)$, $S_B := \text{supp}(x_B^*)$, $I_B := [n] \setminus S_B$. We run standard (FISTA) on the over-regularized (B) problem, and we treat S_A as a region where coordinates are potentially active at every iteration, even if some are inactive for x_B^* . This choice does not entail large work, since the guarantee is $\text{vol}(S_A) \leq 1/\rho$, cf. $\text{vol}(S_B) \leq 1/(2\rho)$.

We also have to account for the work of nodes that are active outside from S_A . Define the spurious active set at step k by $\tilde{A}_k := \text{supp}(x_{k+1}) \cap S_A^c$. Under the degree-weighted work model, such activations are the only mechanism by which FISTA can incur additional locality overhead beyond the cost of working inside S_A . Then, after N iterations, the total degree-weighted work is

$$O\left(N \text{vol}(S_A) + \sum_{k=0}^{N-1} \text{vol}(\tilde{A}_k)\right). \quad (4)$$

The first term corresponds to the cost of running N proximal-gradient steps while remaining in S_A , since computing the gradient and applying the prox map costs work proportional to the volume of the active set. The second term is the cumulative overhead from transient activations outside S_A .

Our goal is to bound (4). The next subsection provides the tools for controlling the second term. In particular, the complementarity-slack lemma (Lemma 4.1) will show that every spurious activation forces a quantitative deviation in the forward-gradient map relative to x_B^* , and the split of Lemma 4.2 will ensure that any index outside S_A has a uniform slack lower bound under the (B) problem. These ingredients remove dependence on tiny margins and allow us to sum the spurious volumes over iterations using FISTA's geometric contraction, leading to our work bound.

4.2 Complementarity slack and spurious activations

We now make precise how momentum-induced activations outside the optimal support can be converted into a quantitative cost that we can later sum over iterations. The main idea is: for a coordinate that is zero at the optimum of the (B) problem, the KKT conditions specify a nontrivial interval in which its (signed) gradient must lie. The distance to the edge of that interval is a measure of how safely inactive the coordinate is. If FISTA nevertheless activates such a coordinate at some extrapolated point, then something must have moved by at least that safety margin. This is the mechanism that will let us bound the cumulative work spent on spurious supports.

Fix the (B) problem and let $x^* := x_B^*$. For every inactive coordinate $i \in I_B$, define its degree-normalized complementarity (KKT) slack by

$$\gamma_i := \frac{\lambda_i - |\nabla f(x^*)_i|}{\sqrt{d_i}} = \frac{\lambda_i + \nabla_i f(x^*)}{\sqrt{d_i}} \geq 0, \quad \text{where } \lambda_i := 2\alpha\rho\sqrt{d_i}. \quad (5)$$

The quantity γ_i is the (degree-normalized) gap between the soft-threshold level λ_i and the magnitude of the optimal gradient at coordinate i . In other words, it measures how far coordinate i is from becoming active at the optimum. Define the gradient map and the set of spurious nodes by

$$u(x) := x - \eta\nabla f(x), \quad A(y) := \text{supp}(\text{prox}_{\eta g_B}(u(y))) \cap I_B \quad \text{for any } x \in \mathbb{R}^n, y \in \mathbb{R}^n.$$

Here $u(\cdot)$ is the standard forward step used by proximal-gradient methods, and $A(y)$ is the subset of (B)-inactive indices that become nonzero after applying the prox map at the point y . The set $A(y_k)$ is exactly what creates the extra per-iteration cost due to spurious exploration with respect to an ideal local acceleration complexity of $\tilde{O}(1/(\rho\sqrt{\alpha}))$.

We now formalize the connection between a spurious activation and a nontrivial deviation in the forward step. This is the basic bridge from optimality structure to the work bound.

Lemma 4.1 [\Downarrow] Fix $y \in \mathbb{R}^n$. For every $i \in A(y)$, $|u(y)_i - u(x^*)_i| > \eta \gamma_i \sqrt{d_i}$.

Lemma 4.1 is what allows us to turn spurious activations into a summable error budget that is compatible with FISTA's convergence rate, given that the distance to optimizer bounds $\|u(y_k) - u(x^*)\|$ and contracts with time. Recall that the margin for the (B) problem can be written as

$$\gamma_i^{(B)} := 2\rho\alpha + \frac{\nabla_i f(x_B^*)}{\sqrt{d_i}} \quad \text{for } i \in I_B. \quad (6)$$

We now show that the margin of coordinates that are not in S_A is large enough.

Lemma 4.2 [\Downarrow] Let $I_B := [n] \setminus S_B$ be the inactive set for problem (B), and define

$$I_B^{\text{small}} := \left\{ i \in I_B : \gamma_i^{(B)} < \rho\alpha \right\}, \quad I_B^{\text{large}} := \left\{ i \in I_B : \gamma_i^{(B)} \geq \rho\alpha \right\}.$$

Then $I_B^{\text{small}} \subseteq S_A$.

Next, we compute a bound on the work $\text{vol}(\tilde{A}_k)$ which is proportional to the inverse minimum margin of the coordinates involved, and this quantity is no more than $1/(\rho\alpha)$ by the lemma above.

4.3 Work bound and sufficient conditions

We now derive a bound on the work. Recall the decomposition (4), the uniform bound for the margin of coordinates in \tilde{A}_k in the previous section, together with Cauchy-Schwarz and the distance contraction of $\|y_k - x_B^*\|_2$ that we show in Corollary A.3, makes the series $\sum_k \text{vol}(\tilde{A}_k)$ summable and leads to the overhead term in the theorem below.

Theorem 4.3 [\Downarrow] For the (B) problem with objective $F_B(x) = f(x) + g_B(x)$, run (FISTA). Let \mathcal{B} be a set such that $\tilde{A}_k \subseteq \mathcal{B}$ for all $k \geq 0$. Then, we reach $F_B(x_N) - F_B(x_B^*) \leq \varepsilon$ after a total degree-weighted work of at most

$$\text{Work}(N_\varepsilon) \leq O\left(\frac{1}{\rho\sqrt{\alpha}} \log\left(\frac{\alpha}{\varepsilon}\right) + \frac{\sqrt{\text{vol}(\mathcal{B})}}{\rho\alpha^{3/2}}\right).$$

The bound in Theorem 4.3 separates the cost of converging on S_A , from the extra cost of transient exploration. The first term is the baseline accelerated contribution: FISTA needs $N_\varepsilon = O((\sqrt{\alpha})^{-1} \log(\alpha/\varepsilon))$ iterations, and each iteration costs at most a constant times $\text{vol}(S_A) \leq 1/\rho$, yielding $O((\rho\sqrt{\alpha})^{-1} \log(\alpha/\varepsilon))$. The second term bounds the entire cumulative volume of the spurious sets \tilde{A}_k . The factor $\rho^{-1}\alpha^{-3/2}$ reflects the combination of (i) the uniform margin $\rho\alpha$ obtained from Lemma 4.2 and (ii) the geometric contraction of the iterates, which sums to $O(\alpha^{-1/2})$.

We used hypothesis $\tilde{A}_k \subseteq \mathcal{B}$ as an explicit locality requirement. We now give a checkable graph-structural sufficient condition that implies such confinement, with \mathcal{B} identified as a vertex boundary.

Theorem 4.4 [\Downarrow] Consider the (B) problem objective $F_{2\rho}$ in (RPPR), and let S be a set such that $S_B \subseteq S$. Define ∂S as the vertex boundary of S and $\text{Ext}(S) := V \setminus (S \cup \partial S)$. Assume there exists $\xi \in [0, 1]$ such that for all $i \in \text{Ext}(S)$,

$$\frac{|\mathcal{N}(\{i\}) \cap \partial S|}{d_i} \leq \left(\frac{\alpha\rho}{2(1-\alpha)}\right)^2 d_i d_{\min \partial S}, \quad (7)$$

where $d_{\min \partial S} := \min_{j \in \partial S} d_j$. Then the iterates of (FISTA) satisfy, for all $k \geq 0$:

$$\text{supp}(x_k) \subseteq S \cup \partial S.$$

Theorem 4.4 provides a mechanism by which spurious activations can be ruled out in the exterior of a candidate region. Condition (7) controls how an exterior node is connected to the current active region by upper-bounding the fraction of its incident edges that connect to the boundary ∂S . This condition is favorable for FISTA: it rules out ‘‘percolation’’ of extrapolated iterates into the exterior. Nevertheless, our synthetic experiments in Section 5 still exhibit regimes where FISTA is slower.

Remark 4.5 If $S = S_A$ in Theorem 4.4, then $\text{supp}(x_k) \subseteq S_A \cup \partial S_A$ for all $k \geq 0$. So any spurious activation happens in $\mathcal{B} := \partial S_A$, that is, the confinement hypothesis in Theorem 4.3 holds with $\mathcal{B} = \partial S_A$, and the overhead term in the work bound is governed by the boundary volume $\text{vol}(\partial S_A)$.

Remark 4.6 In Section B, we prove a complementary property showing that nodes of high-enough degree do not every get activated, which implies in fact the $\text{vol}(\mathcal{B})$ term in Theorem 4.3 can be reduced to the volume of nodes in \mathcal{B} with degree below a threshold given by the amount in Section B.

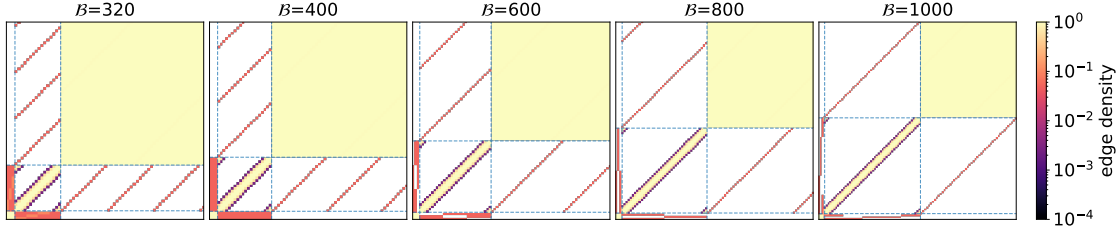


Figure 1: *Adjacency density*. For each boundary size $|\mathcal{B}|$ we visualize the adjacency matrix via a binned edge-density heatmap (bin size 20), where each pixel shows the fraction of possible edges between a pair of bins (log-scaled; colormap magma with white below 10^{-4}). Dashed lines mark the core | boundary | exterior block boundaries. The plots show the clique (upper-left block), the boundary circulant band, the nearly dense exterior block, and the sparse cross-region interfaces.

5 Experiments

This section evaluates when FISTA reduces (and when it can increase) the total degree-weighted work for ℓ_1 -regularized PageRank, reflecting the tradeoff in [Theorem 4.3](#). We present two sets of experiments. First, we consider a controlled synthetic core-boundary-exterior graph family. Details on parameter tuning are given in [Section D](#). Second, we compare ISTA and FISTA on real data: SNAP [\[LK14\]](#) graphs. In our experiments, we did not over-regularize the problem.

For synthetic experiments the no-percolation assumption is satisfied. We use a three-block node partition $V = S \cup \mathcal{B} \cup \text{Ext}$, where S (the core) contains the seed. The induced subgraph on S is a clique, while \mathcal{B} (the boundary) and Ext (the exterior) are each internally connected. Cross-region connectivity is sparse: the core connects to \mathcal{B} with a fixed per-core fan-out, and each exterior node has one neighbor in \mathcal{B} . This yields a clear block structure in the adjacency matrix and lets us vary the boundary size/volume $\text{vol}(\mathcal{B})$ while keeping the core fixed. [Figure 1](#) visualizes an example of this construction. We provide details in [Section D](#)³.

5.1 Synthetic boundary-volume sweep experiment

This section provides synthetic experiments illustrating how the boundary volume can dominate the running time of accelerated proximal-gradient methods. In particular, the experiment isolates the mechanism behind the $\sqrt{\text{vol}(\mathcal{B})}$ -term in the work bound in [Theorem 4.3](#), and shows empirically that, as $\text{vol}(\mathcal{B})$ increases, the accelerated method can become slower than its non-accelerated counterpart.

We use the core-boundary-exterior synthetic construction from [Section 5](#), and vary only the boundary size $|\mathcal{B}|$ (and hence $\text{vol}(\mathcal{B})$), keeping the core, exterior, and all degree/connectivity parameters fixed. On each instance of the sweep we solve the ℓ_1 -regularized PageRank objective (RPPR) with $\alpha = 0.20$ and $\rho = 10^{-4}$, comparing ISTA and FISTA under the common initialization, parameter choices, stopping protocol, and degree-weighted work accounting described in [Section 5](#). We set $\varepsilon = 10^{-6}$.

[Figure 2](#) plots the work to reach the common stopping target as a function of $\text{vol}(\mathcal{B})$. The key trend is that FISTA becomes increasingly expensive as $\text{vol}(\mathcal{B})$ grows. For sufficiently large $\text{vol}(\mathcal{B})$ it becomes slower than ISTA.

This is exactly the behavior suggested by the bound in [Theorem 4.3](#) (and in particular by the $\sqrt{\text{vol}(\mathcal{B})}/(\rho\alpha^{3/2})$ term): as the boundary volume grows, the potential cost of spurious exploration in the boundary grows as well.

5.2 Sweeps in ρ , α and ε at fixed boundary size

We fix $|\mathcal{B}| = 600$, and we run three sweeps (summarized in [Figure 3](#)): (i) an ρ -sweep, reported for both a dense-core (clique) instance and a sparse-core variant (connected, 20% of clique edges) to confirm that the observed ρ -dependence

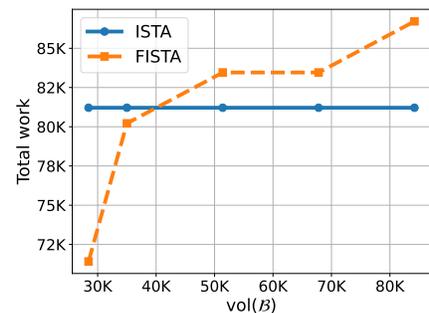


Figure 2: *Work vs. vol(B)*. Work by ISTA and FISTA against $\text{vol}(\mathcal{B})$.

³Code that reproduces all experiments is available at https://github.com/watcl-lab/accelerated_l1_PageRank_experiments.

is not an artifact of the symmetric clique core; (ii) an α -sweep with $\rho = 10^{-4}$; and (iii) an ε -sweep at fixed $\alpha = 0.20$ (complete details in Section E).

The ρ sweeps (Figures 3a and 3b) show that work decreases as ρ increases and collapses to 0 beyond the trivial-solution threshold; across the sweep, ISTA and FISTA exhibit qualitatively similar $1/\rho$ -type scaling, consistent with the ρ -dependence in Theorem 4.3 for fixed α and fixed boundary size. The α sweep (Figure 3c) shows increasing work as α decreases, and FISTA can be slower than ISTA over a substantial small- α range, consistent with the interpretation of Theorem 4.3. Finally, the ε sweep (Figure 3d) shows increasing work as the tolerance decreases. FISTA is faster for small ε , consistent with the interpretation of Theorem 4.3.

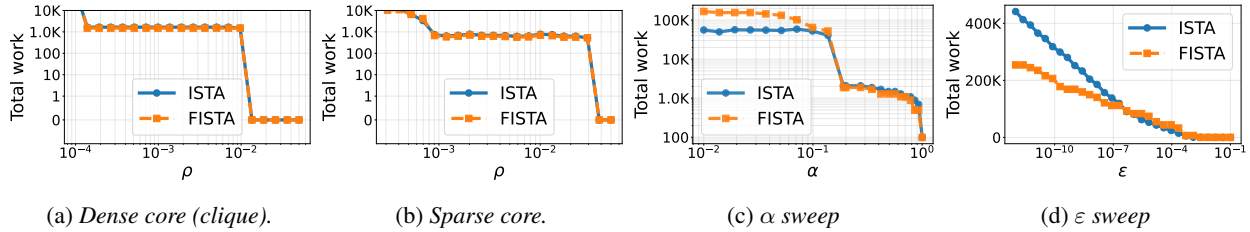


Figure 3: Sweeps at fixed $|\mathcal{B}| = 600$. Figure 3a shows the ρ -sweep with a dense core (clique) on a fresh randomized graph per ρ ; Figure 3b shows the ρ -sweep with a sparse core (connected, 20% of clique edges) on a fresh randomized graph per ρ . Figure 3c sweeps α at a fixed residual tolerance $\varepsilon = 10^{-6}$ on a single instance constructed to satisfy $\xi > 0$ and the no-percolation condition at the smallest swept value, with parameters selected by an inexpensive auto-tuning step (Section E). Figure 3d sweeps the tolerance ε at fixed $\alpha = 0.20$ on the baseline unweighted instance.

5.3 Real-data benchmarks on SNAP graphs

Our synthetic experiments use a deliberate core-boundary-exterior construction in order to satisfy the no-percolation assumption. The real-data benchmarks in this subsection are at the opposite end of the spectrum: heterogeneous SNAP [LK14] networks whose connectivity and degree profiles are not engineered to fit the synthetic template. We include these datasets to illustrate both a positive and a negative real example for acceleration. On `com-Amazon`, `com-DBLP`, and `com-Youtube` we typically observe a consistent work reduction with FISTA, whereas `com-Orkut` exhibits a setting where FISTA can be slower due to costly exploration beyond the optimal support.⁴

Work vs. parameter α . We sweep α over a log-spaced grid in $[10^{-3}, 0.9]$ while fixing $\rho = 10^{-4}$ and $\varepsilon = 10^{-85}$; results are in Figure 4. On `com-Amazon`, `com-DBLP`, and `com-Youtube`, FISTA consistently reduces work relative to ISTA across the full α range. On `com-Orkut`, however, FISTA can be slower than ISTA for small α before becoming competitive again at moderate and large α , illustrating that acceleration can lose under our work metric.

Work vs. KKT tolerance ε . We next fix $\alpha = 0.20$ and $\rho = 10^{-4}$ and sweep the tolerance ε over a log-spaced grid in $[10^{-8}, 10^{-2}]$; results are in Figure 5. Tightening the tolerance (smaller ε) increases work for both methods, and FISTA typically achieves the same tolerance with less total work on these datasets, though the gap can be small (notably on `com-Orkut`) for intermediate tolerances.

Work vs. sparsity parameter ρ . Finally, we fix $\alpha = 0.20$ and $\varepsilon = 10^{-8}$ and sweep ρ over a log-spaced grid in $[10^{-6}, 10^{-2}]$; results are shown in Figure 6. As ρ increases (stronger regularization), the solutions become more localized and the work decreases sharply. Across all four graphs, FISTA generally improves upon ISTA by a modest constant factor for these settings.

Additional diagnostics. Because total work conflates iteration count and per-iteration cost, aggregate curves alone do not explain why the ISTA–FISTA ranking differs across datasets. In Section F we separate these two factors and we report degree-tail summaries. In particular, the diagnostics show that `com-Orkut`’s slowdowns are driven by costly transient exploration, i.e., small sets of high-degree activations inflate the per-iteration work and can offset (or even reverse) the iteration savings of acceleration (Figures 7 and 8).

⁴For each dataset we sample 300 seed nodes uniformly at random from the non-isolated vertices; the same seed set is reused for both ISTA and FISTA and across all sweeps. In the sweep plots below, solid lines are means over the 300 seeds and the shaded bands show the interquartile range (25%-75%).

⁵Note that $\varepsilon = 10^{-8}$ is different from the value used in the synthetic experiments, which was $\varepsilon = 10^{-6}$. This is because we observed that the latter setting was too large for the real data to produce meaningful plots.

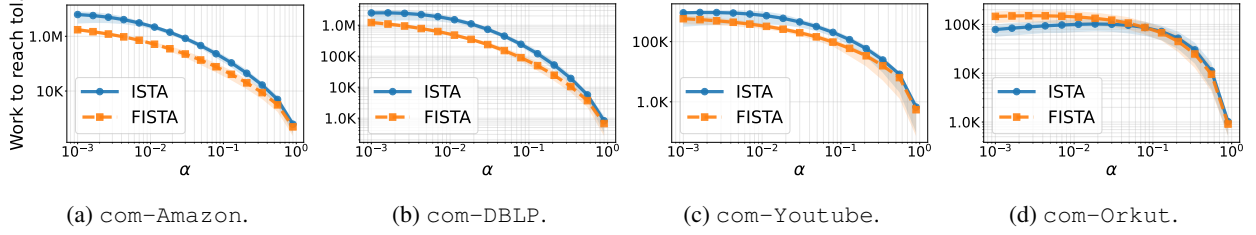


Figure 4: *Real graphs: work vs. α* . Work to reach tolerance 10^{-8} as a function of α , with $\rho = 10^{-4}$ fixed. Curves show mean over 300 random seeds; shaded bands are interquartile ranges.

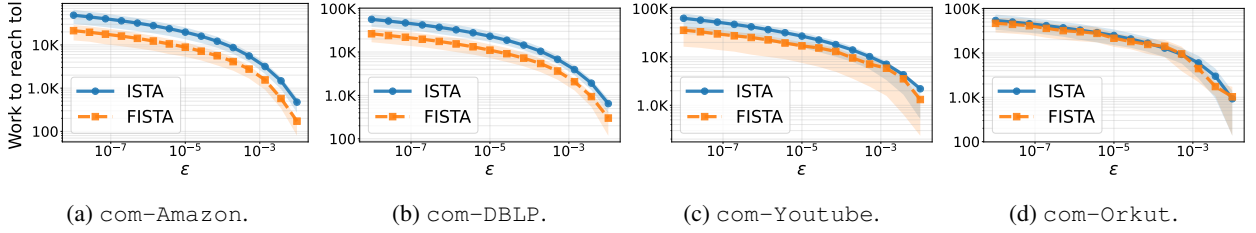


Figure 5: *Real graphs: work vs. KKT tolerance*. Work to reach ϵ , with $\alpha = 0.20$ and $\rho = 10^{-4}$ fixed. Curves show mean over 300 random seeds; shaded bands are interquartile ranges.

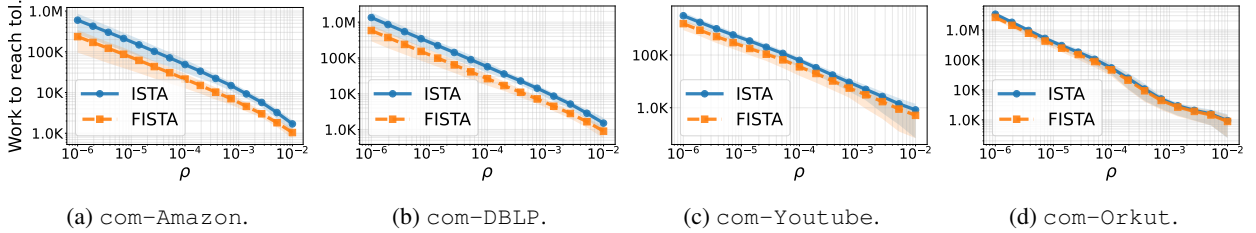


Figure 6: *Real graphs: work vs. ρ* . Work to reach 10^{-8} as a function of ρ , with $\alpha = 0.20$ fixed. Curves show mean over 300 random seeds; shaded bands are interquartile ranges.

6 Conclusion, limitations and future work

We analyzed the classical one-gradient-per-iteration accelerated proximal-gradient method (FISTA) for ℓ_1 -regularized PageRank under a degree-weighted locality work model. Under a verifiable confinement assumption, the resulting complexity decomposes into acceleration together with an explicit overhead that quantifies momentum-induced transient exploration. The main limitation is that the bound is informative when spurious activations remain confined to a boundary set of moderate volume. Several directions remain open. For example, establishing lower bounds in the degree-weighted work model. Additional work could sharpen confinement diagnostics and derive more instance-adaptive predictions, as well as extend the framework to other acceleration schemes.

Acknowledgements

K. Fountoulakis would like to acknowledge the support of the Natural Sciences and Engineering Research Council of Canada (NSERC). Cette recherche a été financée par le Conseil de recherches en sciences naturelles et en génie du Canada (CRSNG), [RGPIN-2019-04067, DGECR-2019-00147].

D. Martínez-Rubio was partially funded by grant PID2024-160448NA-I00 and by La Caixa Junior Leader Fellowship 2025.

References

- [ACL06] Reid Andersen, Fan R. K. Chung, and Kevin J. Lang. [Local Graph Partitioning using PageRank Vectors](#). In: *47th Annual IEEE Symposium on Foundations of Computer Science (FOCS 2006), 21-24 October 2006, Berkeley, California, USA, Proceedings*. IEEE Computer Society, 2006, pp. 475–486 (cit. on pp. 1–3).
- [BC14] Steve E. Butler and Fan R. K. Chung. [Spectral Graph Theory](#). In: *Handbook of Linear Algebra*. Ed. by Leslie Hogben. 2nd. Boca Raton, FL, USA: CRC Press, 2014, pp. 47-1–47-14. ISBN: 9781466507289 (cit. on p. 3).
- [Bec17] Amir Beck. *First-Order Methods in Optimization*. Vol. 25. MOS-SIAM Series on Optimization. Philadelphia, PA, USA: Society for Industrial and Applied Mathematics (SIAM), 2017. ISBN: 9781611974980 (cit. on p. 12).
- [BI20] Gilles Bareilles and Franck Iutzeler. [On the interplay between acceleration and identification for the proximal gradient algorithm](#). In: *Computational Optimization and Applications* 77 (2020), pp. 351–378 (cit. on p. 3).
- [BM94] James V. Burke and Jorge J. Moré. [Exposing Constraints](#). In: *SIAM J. Optim.* 4.3 (1994) (cit. on p. 3).
- [BT09] Amir Beck and Marc Teboulle. [A Fast Iterative Shrinkage-Thresholding Algorithm for Linear Inverse Problems](#). In: *SIAM J. Imaging Sci.* 2.1 (2009) (cit. on pp. 1, 4).
- [FRS+19] Kimon Fountoulakis, Farbod Roosta-Khorasani, Julian Shun, Xiang Cheng, and Michael W Mahoney. [Variational perspective on local graph clustering](#). In: *Mathematical Programming* 174.1 (2019), pp. 553–573 (cit. on pp. 1–4, 12, 14).
- [FY22] Kimon Fountoulakis and Shenghao Yang. [Open Problem: Running time complexity of accelerated \$\ell_1\$ -regularized PageRank](#). In: *Proceedings of Thirty Fifth Conference on Learning Theory*. Vol. 178. Proceedings of Machine Learning Research. PMLR, 2022, pp. 5630–5632 (cit. on p. 3).
- [Gar20] Dan Garber. [Revisiting Frank-Wolfe for Polytopes: Strict Complementarity and Sparsity](#). In: *Advances in Neural Information Processing Systems 33: Annual Conference on Neural Information Processing Systems 2020, NeurIPS 2020*. Ed. by Hugo Larochelle, Marc’Aurelio Ranzato, Raia Hadsell, Maria-Florina Balcan, and Hsuan-Tien Lin. 2020 (cit. on p. 3).
- [Gle15] David F. Gleich. [PageRank Beyond the Web](#). In: *SIAM Review* 57.3 (2015), pp. 321–363 (cit. on pp. 1–3).
- [GM14] David Gleich and Michael Mahoney. [Anti-differentiating approximation algorithms: A case study with min-cuts, spectral, and flow](#). In: *Proceedings of the 31st International Conference on Machine Learning*. Vol. 32. Proceedings of Machine Learning Research 2. PMLR, 2014, pp. 1018–1025 (cit. on pp. 1, 2).
- [GM86] Jacques Guélat and Patrice Marcotte. [Some comments on Wolfe’s ‘away step’](#). In: *Math. Program.* 35 (1986), pp. 110–119 (cit. on p. 3).
- [HFM21] Wooseok Ha, Kimon Fountoulakis, and Michael W. Mahoney. [Statistical guarantees for local graph clustering](#). In: *Journal of Machine Learning Research* 22.148 (2021), pp. 1–54 (cit. on pp. 2, 3, 12).
- [LK14] Jure Leskovec and Andrej Krevl. *SNAP Datasets: Stanford Large Network Dataset Collection*. <http://snap.stanford.edu/data>. June 2014 (cit. on pp. 2, 7, 8).
- [MWP23] David Martínez-Rubio, Elias Wirth, and Sebastian Pokutta. [Accelerated and Sparse Algorithms for Approximate Personalized PageRank and Beyond](#). In: *Proceedings of Thirty Sixth Conference on Learning Theory*. Vol. 195. Proceedings of Machine Learning Research. PMLR, 2023, pp. 2852–2876 (cit. on p. 3).

- [Nes04] Yurii Nesterov. *Introductory Lectures on Convex Optimization: A Basic Course*. Vol. 87. Applied Optimization. Springer, 2004. ISBN: 978-1-4020-7553-7 (cit. on p. 1).
- [NSH19] Julie Nutini, Mark Schmidt, and Warren Hare. [Active-Set Complexity of Proximal Gradient: How Long Does It Take to Find the Sparsity Pattern?](#) In: *Optimization Letters* 13 (2019), pp. 645–655 (cit. on p. 3).
- [SJN+19] Yifan Sun, Halyun Jeong, Julie Nutini, and Mark Schmidt. [Are we there yet? Manifold identification of gradient-related proximal methods.](#) In: *Proceedings of the Twenty-Second International Conference on Artificial Intelligence and Statistics*. Vol. 89. Proceedings of Machine Learning Research. PMLR, 2019, pp. 1110–1119 (cit. on p. 3).
- [Wol70] Philip Wolfe. [Convergence Theory in Nonlinear Programming.](#) In: *Integer and Nonlinear Programming*. Ed. by J. Abadie. Amsterdam, Netherlands: North-Holland Publishing Company, 1970, pp. 1–36. ISBN: 9780444100009 (cit. on p. 3).
- [ZSB+24] Baojian Zhou, Yifan Sun, Reza Babanezhad Harikandeh, Xingzhi Guo, Deqing Yang, and Yanghua Xiao. [Iterative Methods via Locally Evolving Set Process.](#) In: *Advances in Neural Information Processing Systems*. Vol. 37. Curran Associates, Inc., 2024, pp. 141528–141586 (cit. on p. 3).

A Proofs

Lemma A.1 (Initial gap) Assume the seed is a single node v so $s = e_v$ and initialize $x_0 = 0$. Then $F_\rho(0) = 0$ and

$$\Delta_0 = F_\rho(0) - F_\rho(x^*) = -F_\rho(x^*) \leq \frac{\alpha}{2d_v} \leq \frac{\alpha}{2}.$$

Proof We have $F_\rho(x) \geq f(x)$ and thus $F_\rho(x^*) \geq \min_x f(x)$. The unconstrained minimizer of the quadratic f is $x_f^* = Q_f^{-1}b$ and $\min f = -\frac{1}{2}b^\top Q_f^{-1}b$. Because $Q \succeq \alpha I$, we have $Q_f^{-1} = Q^{-1} \preceq \frac{1}{\alpha}I$, and therefore

$$b^\top Q_f^{-1}b \leq \frac{1}{\alpha}b^\top b = \frac{1}{\alpha}\alpha^2\|D^{-1/2}s\|_2^2 = \alpha s^\top D^{-1}s.$$

For $s = e_v$, we have $s^\top D^{-1}s = 1/d_v$, which yields

$$\min f \geq -\frac{\alpha}{2d_v}, \quad \text{and hence} \quad -F_\rho(x^*) \leq -\min f \leq \frac{\alpha}{2d_v}. \quad \blacksquare$$

We now state the classical guarantee on the function-value convergence on FISTA.

Fact A.2 (FISTA convergence rate) Assume f is L -smooth and F is μ -strongly convex with respect to $\|\cdot\|_2$. Run (FISTA) with $\eta = 1/L$ and $\beta := \frac{\sqrt{L/\mu-1}}{\sqrt{L/\mu+1}} \in [0, 1)$. Then

$$F(x_k) - F(x^*) \leq 2(F(x_0) - F(x^*)) \left(1 - \sqrt{\frac{\mu}{L}}\right)^k \quad \text{for all } k \geq 1.$$

See [Bec17, Section 10.7.7] and take into account that $\frac{\mu}{2}\|x_0 - x^*\|_2^2 \leq F(x_0) - F(x^*)$ by strong convexity. We note that the convergence guarantee above, along with strong convexity, yields bounds on the distance to the minimizer x^* .

As a corollary, we can bound the distance to optimizer of the iterates along the whole computation path.

Corollary A.3 (FISTA iterates) In the setting of Fact A.2, we have:

$$\|y_0 - x^*\|_2^2 \leq \frac{4\Delta_0}{\mu} \quad \text{and} \quad \|y_k - x^*\|_2^2 \leq M \left(1 - \sqrt{\frac{\mu}{L}}\right)^{k-1} \quad \text{for all } k \geq 1,$$

for $M := \frac{8\Delta_0}{\mu} \left((1 + \beta)^2(1 - \sqrt{\mu/L}) + \beta^2\right)$.

Using the bounds on Δ_0 and μ in Section 3, one obtains that for (RPPR) it is $M \leq 20$ and $\Delta_0/\mu \leq 1/2$. Thus $\|y_k - x^*\|_2 \leq \sqrt{20}$ for all $k \geq 0$.

Proof Let $q := 1 - \sqrt{\mu/L}$. Strong convexity gives $F(x) - F(x^*) \geq \frac{\mu}{2}\|x - x^*\|_2^2$, hence, by Fact A.2:

$$\|x_k - x^*\|_2^2 \leq \frac{2}{\mu}(F(x_k) - F(x^*)) \leq \frac{4\Delta_0}{\mu}q^k,$$

which already yields the result for $k = 0$, using $y_0 = x_0$. For $k \geq 1$, write $y_k - x^* = (1 + \beta)(x_k - x^*) - \beta(x_{k-1} - x^*)$ and use $\|a - b\|_2^2 \leq 2\|a\|_2^2 + 2\|b\|_2^2$ to obtain

$$\|y_k - x^*\|_2^2 \leq 2(1 + \beta)^2\|x_k - x^*\|_2^2 + 2\beta^2\|x_{k-1} - x^*\|_2^2.$$

Substitute the bounds on $\|x_k - x^*\|_2^2$ and $\|x_{k-1} - x^*\|_2^2$. \blacksquare

Proof of Lemma 4.1. Fix $i \in A(y) \subseteq I^*$. Then $x_i^* = 0$, and we have

$$|u(y)_i - u(x^*)_i| \stackrel{\textcircled{1}}{\geq} \|u(y)_i - |u(x^*)_i|\| \geq |u(y)_i| - |u(x^*)_i| \stackrel{\textcircled{2}}{>} \eta\lambda_i - \eta(\lambda_i - \gamma_i\sqrt{d_i}) = \eta\gamma_i\sqrt{d_i}.$$

where we used the reverse triangle inequality in $\textcircled{1}$. In $\textcircled{2}$ we used that $i \in A(y)$ means $\text{prox}_{\eta g}(u(y))_i \neq 0$ and so $|u(y)_i| > \eta\lambda_i$. And also that by definition, we have $|u(x^*)_i| = \eta|\nabla f(x^*)_i| = \eta(\lambda_i - \gamma_i\sqrt{d_i})$ by the definition of γ_i . \blacksquare

The following Lemma A.4 is proved, for example, as Lemma 4 in Ha, Fountoulakis, and Mahoney [HFM21] (see also the discussion of regularization paths in Fountoulakis et al. [FRS+19]).

Lemma A.4 (Monotonicity of the ℓ_1 -regularized PageRank path) For the family (RPPR), let $x^*(\rho) := \arg \min_x F_\rho(x)$, for any $\rho > 0$. The solution path is monotone: if $\rho' > \rho \geq 0$, then

$$x^*(\rho') \leq x^*(\rho) \quad \text{coordinatewise.}$$

Lemma A.5 (Monotonicity of proximal gradient steps for PageRank) If $z \geq z' \geq 0$, then

$$\text{prox}_{g_c} \left(z - \frac{1}{L} \nabla f(z) \right) \geq \text{prox}_{g_c} \left(z' - \frac{1}{L} \nabla f(z') \right) \quad (\text{componentwise}).$$

Proof Using the definition of the forward-gradient map $u(z) := z - \frac{1}{L} \nabla f(z)$, and that, for PageRank, $\nabla f(z) = Qz - b$ with $b = \alpha D^{-1/2} s$, we have

$$u(z) = z - \frac{1}{L} (Qz - b) = \left(I - \frac{1}{L} Q \right) z + \frac{1}{L} b.$$

Since Q is an M -matrix (positive semidefinite and off-diagonal entries are nonpositive) and $Q \preceq LI$ (by L -smoothness), the matrix $I - \frac{1}{L} Q$ is entrywise nonnegative. Therefore $u(\cdot)$ is monotone componentwise: $z \geq z' \Rightarrow u(z) \geq u(z')$.

Next, for $g_c(x) = c\alpha \|D^{1/2}x\|_1$, the proximal map is separable and monotone componentwise, since

$$\left(\text{prox}_{g_c}(w) \right)_i = \text{sign}(w_i) \max\{|w_i| - c\alpha\sqrt{d_i}, 0\}.$$

Composing these two monotone maps yields the claim. ■

Proof of Lemma 4.2. Fix any $i \in I_B^{\text{small}} \subseteq I_B$. Then $x_{B,i}^* = 0$. Recall that $u(z) := z - \nabla f(z)$ (here $\eta = 1$).

By the definition (6) of the (B)-margin at coordinate i and the fact that $x_{B,i}^* = 0$, we have

$$\begin{aligned} \gamma_i^{(B)} < \rho\alpha &\iff 2\rho\alpha + \frac{\nabla_i f(x_B^*)}{\sqrt{d_i}} < \rho\alpha \\ &\iff \frac{\nabla_i f(x_B^*)}{\sqrt{d_i}} < -\rho\alpha \\ &\iff \nabla_i f(x_B^*) < -\rho\alpha\sqrt{d_i} \\ &\iff -\nabla_i f(x_B^*) > \rho\alpha\sqrt{d_i} \\ &\iff u(x_B^*)_i > \rho\alpha\sqrt{d_i}. \end{aligned}$$

Therefore, applying the coordinate formula for the prox of g_A (cf. (2)) gives

$$\left(\text{prox}_{g_A}(u(x_B^*)) \right)_i = \text{sign}(u(x_B^*)_i) \max\{|u(x_B^*)_i| - \rho\alpha\sqrt{d_i}, 0\} > 0.$$

Next, since $\rho_B = 2\rho > \rho_A = \rho$, path monotonicity Lemma A.4 yields $x_A^* \geq x_B^*$ componentwise. Applying Lemma A.5 with $c = 1$ (i.e., g_A), $z = x_A^*$, and $z' = x_B^*$, we obtain

$$\text{prox}_{g_A}(u(x_A^*)) \geq \text{prox}_{g_A}(u(x_B^*)) \quad (\text{componentwise}).$$

Finally, x_A^* is a fixed point of the proximal-gradient map for the (A) problem, so $x_A^* = \text{prox}_{g_A}(u(x_A^*))$. Hence

$$x_{A,i}^* = \left(\text{prox}_{g_A}(u(x_A^*)) \right)_i \geq \left(\text{prox}_{g_A}(u(x_B^*)) \right)_i > 0,$$

which implies $i \in \text{supp}(x_A^*) = S_A$. Therefore $I_B^{\text{small}} \subseteq S_A$. ■

Proof of Theorem 4.3. Recall that $\tilde{A}_k = \text{supp}(x_{k+1}) \cap S_A^c$ and that we assume $\tilde{A}_k \subseteq \mathcal{B}$ for all $k \geq 0$. By Lemma 4.2, any index in \tilde{A}_k is (B)-inactive with margin at least $\rho\alpha$; concretely, $\gamma_i^{(B)} \geq \rho\alpha$ for all $i \in \tilde{A}_k$. Let \mathcal{B}' be the subset of \mathcal{B} such that $\gamma_i^{(B)} \geq \rho\alpha$ for all $i \in \mathcal{B}'$. Thus, $\tilde{A}_k \subseteq \mathcal{B}'$.

We first bound the total spurious work:

$$\begin{aligned}
\sum_{k=0}^{\infty} \sum_{i \in \tilde{A}_k} d_i &= \sum_{k=0}^{\infty} \sum_{i \in \tilde{A}_k} \left(\frac{\sqrt{d_i}}{\gamma_i^{(B)}} \right) \left(\gamma_i^{(B)} \sqrt{d_i} \right) \\
&\leq \sum_{k=0}^{\infty} \sqrt{\sum_{i \in \mathcal{B}'} \frac{d_i}{(\gamma_i^{(B)})^2}} \sqrt{\sum_{i \in \tilde{A}_k} (\gamma_i^{(B)})^2 d_i} \quad (\text{Cauchy-Schwarz, and } \tilde{A}_k \subseteq \mathcal{B}') \\
&\leq \sum_{k=0}^{\infty} \sqrt{\sum_{i \in \mathcal{B}'} \frac{d_i}{\rho^2 \alpha^2}} \sqrt{\sum_{i \in \tilde{A}_k} |u(y_k)_i - u(x_B^*)_i|^2} \quad (\text{since } \gamma_i^{(B)} \geq \rho\alpha, \text{ Lemma 4.1}) \\
&\leq \sum_{k=0}^{\infty} \frac{\sqrt{\text{vol}(\mathcal{B})}}{\rho\alpha} \|u(y_k) - u(x_B^*)\|_2 \quad (\text{because } \mathcal{B}' \subseteq \mathcal{B}) \\
&\leq \sum_{k=0}^{\infty} \frac{\sqrt{\text{vol}(\mathcal{B})}}{\rho\alpha} (\|y_k - x_B^*\|_2 + \eta \|\nabla f(y_k) - \nabla f(x_B^*)\|_2) \\
&\leq \sum_{k=0}^{\infty} \frac{\sqrt{\text{vol}(\mathcal{B})}}{\rho\alpha} (1 + \eta L) \|y_k - x_B^*\|_2. \quad (\text{by smoothness})
\end{aligned} \tag{8}$$

For RPPR we use $\eta = 1$ and $L = 1$, hence $(1 + \eta L) = 2$. Using [Corollary A.3](#) and writing $q := 1 - \sqrt{\mu/L} = 1 - \sqrt{\alpha}$, we have $\|y_k - x_B^*\|_2 \leq O(1) q^{k/2}$, so the series in (8) sums to $O((1 - q)^{-1}) = O(\alpha^{-1/2})$. Therefore,

$$\sum_{k=0}^{\infty} \text{vol}(\tilde{A}_k) = O\left(\frac{\sqrt{\text{vol}(\mathcal{B})}}{\rho\alpha^{3/2}}\right).$$

Next, we bound the core work. By the sparsity guarantee for RPPR [[FRS+19](#), Theorem 2], $\text{vol}(S_A) \leq 1/\rho$. Thus, after N iterations, the total work is bounded by

$$\text{Work}(N) = O\left(N \text{vol}(S_A) + \sum_{k=0}^{N-1} \text{vol}(\tilde{A}_k)\right) = O\left(\frac{N}{\rho} + \frac{\sqrt{\text{vol}(\mathcal{B})}}{\rho\alpha^{3/2}}\right).$$

Finally, by [Fact A.2](#), to ensure $F_B(x_N) - F_B(x_B^*) \leq \varepsilon$ it suffices to take

$$N \geq N_\varepsilon := \left\lceil \frac{\log(\Delta_0/\varepsilon)}{\log(1/(1 - \sqrt{\mu/L}))} \right\rceil = O\left(\frac{1}{\sqrt{\alpha}} \log\left(\frac{\alpha}{\varepsilon}\right)\right),$$

using $L = 1$, $\mu = \alpha$, and $\Delta_0 \leq \alpha/2$ from [Section 3](#). Substituting $N = N_\varepsilon$ yields the stated bound. \blacksquare

Proof of Theorem 4.4. We prove by induction that $\text{supp}(x_k) \subseteq S \cup \partial S$ for all $k \geq 0$. The base case is trivial, since $x_0 = 0$, so $\text{supp}(x_0) = \emptyset \subseteq S \cup \partial S$.

Now assume $\text{supp}(x_{k-1}) \subseteq S \cup \partial S$ and $\text{supp}(x_k) \subseteq S \cup \partial S$ for some $k \geq 0$ (with $x_{-1} = x_0 = 0$ covering $k = 0$). Then $\text{supp}(y_k) \subseteq \text{supp}(x_k) \cup \text{supp}(x_{k-1}) \subseteq S \cup \partial S$.

Fix any $i \in \text{Ext}(S)$. Since $i \notin S \cup \partial S$ and $\text{supp}(y_k) \subseteq S \cup \partial S$, we have $y_{k,i} = 0$. Also $i \neq v$ (the seed lies in S), hence $(D^{-1/2}s)_i = 0$.

For RPPR, $\nabla f(y) = Qy - \alpha D^{-1/2}s$, so with $\eta = 1$ we have

$$u(y) = y - \nabla f(y) = (I - Q)y + \alpha D^{-1/2}s.$$

Using $Q = \frac{1+\alpha}{2}I - \frac{1-\alpha}{2}D^{-1/2}AD^{-1/2}$, we get $(I - Q) = \frac{1-\alpha}{2}(I + D^{-1/2}AD^{-1/2})$. Therefore, for our fixed $i \in \text{Ext}(S)$,

$$u(y_k)_i = \frac{1-\alpha}{2} \sum_{j \sim i} \frac{y_{k,j}}{\sqrt{d_i d_j}} = \frac{1-\alpha}{2} \sum_{j \in \mathcal{N}(\{i\}) \cap \partial S} \frac{y_{k,j}}{\sqrt{d_i d_j}},$$

because i has no neighbors in S (by definition of $\text{Ext}(S)$) and y_k has no support outside $S \cup \partial S$. Taking absolute values and using $d_j \geq d_{\min \partial S}$ for $j \in \partial S$ gives

$$\begin{aligned} |u(y_k)_i| &\leq \frac{1-\alpha}{2\sqrt{d_i}} \sum_{j \in \mathcal{N}(\{i\}) \cap \partial S} \frac{|y_{k,j}|}{\sqrt{d_j}} \stackrel{\textcircled{1}}{\leq} \frac{1-\alpha}{2\sqrt{d_i}} \cdot \frac{\sqrt{|\mathcal{N}(\{i\}) \cap \partial S|}}{\sqrt{d_{\min \partial S}}} \cdot \|y_k\|_2 \\ &\stackrel{\textcircled{2}}{\leq} \frac{\alpha}{4} \rho \sqrt{d_i} (\|y_k - x^*\|_2 + \|x^*\|_2) \stackrel{\textcircled{3}}{\leq} 2\alpha \rho \sqrt{d_i}. \end{aligned}$$

where $\textcircled{1}$ uses Cauchy-Schwarz and $\textcircled{2}$ uses the triangular inequality and our no-percolation assumption (7). Finally $\textcircled{3}$ uses the bound $\|y_k - x^*\|_2 \leq \sqrt{20}$ from Corollary A.3 and $\|x^*\|_2 \leq 1$ from the preliminaries Section 3 and bound the resulting constants to an integer number.

For the (B) problem, the shrinkage threshold is $\lambda_i = 2\alpha\rho\sqrt{d_i}$, so we showed $|u(y_k)_i| \leq \lambda_i$ and thus the proximal update keeps $x_{k+1,i} = 0$ (cf. the coordinate formula (2)). Since this holds for every $i \in \text{Ext}(S)$, we conclude $\text{supp}(x_{k+1}) \subseteq S \cup \partial S$. This completes the induction. \blacksquare

B High-degree nodes do not activate

We provide an extra property of (FISTA). Nodes of high-enough degree can never be activated by the accelerated iterates when we over-regularize. The proof argues that (FISTA) on problem (B) with a large margin prevents high-degree nodes and large margins are guaranteed for coordinates outside from S_A .

Proposition B.1 (Large-degree nodes do not activate) Run (FISTA) on problem (B) $F_{2\rho}$ and let i such that that the minimizer of problem (A) F_ρ satisfies $x_{A,i}^* = 0$. If

$$d_i \geq \left(\frac{LR}{\alpha\rho} \right)^2,$$

then (FISTA) does not activate node i , that is $x_{k,i} = y_{k,i} = 0$ for all $k \geq 0$.

Using that in our PageRank problem (RPPR), it is $L \leq 1$ and $R \leq 20$, we conclude that nodes satisfying $d_i \geq 1600\alpha^{-2}\rho^{-2}$ will not get activated.

Proof Fix i such that $x_{A,i}^* = 0$. By path monotonicity Lemma A.4 and nonnegativity of the minimizers,

$$\Delta x := x_A^* - x_B^* \geq 0 \quad \text{and} \quad \Delta x_i = 0.$$

Recall $\nabla f(x) = Qx - b$, where $b \geq 0$ and $Q_{ij} \leq 0$ for $i \neq j$. Since $x_A^*, x_B^* \geq 0$ and $x_{A,i}^* = x_{B,i}^* = 0$, we have

$$\nabla_i f(x_A^*) \leq 0, \quad \nabla_i f(x_B^*) \leq 0,$$

and

$$\nabla_i f(x_B^*) - \nabla_i f(x_A^*) = -(Q\Delta x)_i = -\sum_{j \neq i} Q_{ij} \Delta x_j \geq 0.$$

Hence

$$|\nabla_i f(x_B^*)| \leq |\nabla_i f(x_A^*)| \leq \alpha\rho\sqrt{d_i},$$

where the last inequality holds by the KKT conditions for problem (A) (ρ -regularization),

We now prove $x_{k,i} = 0$ for all k by induction. The base case holds since $x_{-1} = x_0 = 0$. Assume $x_{k,i} = x_{k-1,i} = 0$. Then $y_{k,i} = 0$ and by L -smoothness,

$$|\nabla_i f(y_k)| \leq |\nabla_i f(x_B^*)| + \|\nabla f(y_k) - \nabla f(x_B^*)\|_2 \leq \alpha\rho\sqrt{d_i} + L\|y_k - x_B^*\|_2.$$

Using $\|y_k - x_B^*\|_2 \leq R$ and $d_i \geq \left(\frac{LR}{\alpha\rho} \right)^2$, we obtain

$$|\nabla_i f(y_k)| \leq 2\alpha\rho\sqrt{d_i}. \tag{9}$$

Let $w_k = y_k - \eta \nabla f(y_k)$. Since $y_{k,i} = 0$, $|w_{k,i}| = \eta |\nabla_i f(y_k)|$. The proximal map of $g(x) = \alpha \rho \|D^{1/2}x\|_1$ is weighted soft-thresholding, so by (9),

$$x_{k+1,i} = \text{sign}(w_{k,i}) \max\{|w_{k,i}| - 2\eta\alpha\rho\sqrt{d_i}, 0\} = 0.$$

This closes the induction and proves $x_{k,i} = 0$ for all $k \geq 0$. ■

C Bad instances where the margin γ can be very small

We now record two explicit graph families showing that the degree-normalized strict-complementarity margin (the one that naturally interfaces with our degree-weighted work model in (4)) can be made arbitrarily small (and even $\gamma = 0$) by choosing ρ near a breakpoint of the regularization path where an inactive KKT inequality becomes tight. This motivates our theory for linking a problem (B) with the sparsity pattern of a slightly less regularized one (A), so that no requirement in the minimum margin is made (since we split the coordinates into low-margin ones which are included in the support of the (A) solution and then the high-margin ones). Concretely, let x^* be the minimizer and $I^* := \{i : x_i^* = 0\}$. Define the coordinatewise degree-normalized KKT slack

$$\gamma_i := \frac{\lambda_i - |\nabla_i f(x^*)|}{\sqrt{d_i}} \quad (i \in I^*), \quad \lambda_i := \rho\alpha\sqrt{d_i},$$

and the global margin

$$\gamma := \min_{i \in I^*} \gamma_i.$$

C.1 Star graph (seed at the center)

Let G be a star on $m + 1$ nodes with center node c of degree $d_c = m$ and leaves ℓ of degree 1. Let the seed be $s = e_c$.

Lemma C.1 (Star graph breakpoint: γ can be 0) Fix $\alpha \in (0, 1]$ and $m \geq 1$ and define

$$\rho_0 := \frac{1 - \alpha}{2m}.$$

For any $\rho \in [\rho_0, 1/m)$, the unique minimizer has support $S^* = \{c\}$, with

$$x_c^* = \frac{2\alpha(1 - \rho m)}{(1 + \alpha)\sqrt{m}}.$$

Moreover, for any leaf ℓ (recall $d_\ell = 1$), with $\lambda_\ell = \alpha\rho\sqrt{d_\ell} = \alpha\rho$, the degree-normalized slack equals

$$\gamma_\ell := \frac{\lambda_\ell - |\nabla_\ell f(x^*)|}{\sqrt{d_\ell}} = \lambda_\ell - |\nabla_\ell f(x^*)| = \frac{2\alpha}{1 + \alpha} (\rho - \rho_0),$$

and thus at the breakpoint $\rho = \rho_0$ one has $\gamma = 0$.

Proof Recall that $f(x) = \frac{1}{2}x^\top Qx - \alpha \langle D^{-1/2}s, x \rangle$, hence

$$\nabla f(x) = Qx - \alpha D^{-1/2}s,$$

and

$$Q = \alpha I + \frac{1 - \alpha}{2} (I - D^{-1/2}AD^{-1/2}) = \frac{1 + \alpha}{2} I - \frac{1 - \alpha}{2} D^{-1/2}AD^{-1/2}.$$

On the star with seed $s = e_c$, we have $D^{-1/2}s = e_c/\sqrt{m}$, and for each leaf ℓ , $(D^{-1/2}AD^{-1/2})_{\ell c} = 1/\sqrt{m}$. Therefore

$$Q_{cc} = \frac{1 + \alpha}{2}, \quad Q_{\ell c} = Q_{c\ell} = -\frac{1 - \alpha}{2\sqrt{m}}.$$

Assume $x^* = x_c^* e_c$ with $x_c^* > 0$. For the ℓ_1 -regularized PageRank objective $F_\rho(x) = f(x) + \alpha\rho\|D^{1/2}x\|_1 + \mathbb{I}_{\mathbb{R}_{\geq 0}}(x)$, the coordinatewise KKT conditions (cf. (1)) give, at an active coordinate, $\nabla_c f(x^*) = -\alpha\rho\sqrt{d_c} = -\alpha\rho\sqrt{m}$. Using $\nabla_c f(x^*) = (Qx^*)_c - \alpha/\sqrt{m} = Q_{cc}x_c^* - \alpha/\sqrt{m}$, we obtain

$$0 = \nabla_c f(x^*) + \alpha\rho\sqrt{m} = Q_{cc}x_c^* - \frac{\alpha}{\sqrt{m}} + \alpha\rho\sqrt{m} = \frac{1+\alpha}{2}x_c^* - \frac{\alpha}{\sqrt{m}} + \alpha\rho\sqrt{m},$$

which yields

$$x_c^* = \frac{2\alpha(1-\rho m)}{(1+\alpha)\sqrt{m}},$$

and this is positive exactly when $\rho < 1/m$. Now fix any leaf ℓ . Since $x_\ell^* = 0$, the KKT condition requires $\nabla_\ell f(x^*) \in [-\alpha\rho\sqrt{d_\ell}, 0] = [-\alpha\rho, 0]$. Here

$$\nabla_\ell f(x^*) = (Qx^*)_\ell = Q_{\ell c}x_c^* = -\frac{1-\alpha}{2\sqrt{m}}x_c^* \leq 0,$$

so the inactive condition is equivalent to

$$|\nabla_\ell f(x^*)| = \frac{1-\alpha}{2\sqrt{m}}x_c^* \leq \alpha\rho.$$

Substituting the expression for x_c^* and cancelling $\alpha > 0$ gives

$$\frac{1-\alpha}{2\sqrt{m}} \cdot \frac{2\alpha(1-\rho m)}{(1+\alpha)\sqrt{m}} \leq \alpha\rho \iff \frac{(1-\alpha)(1-\rho m)}{(1+\alpha)m} \leq \rho \iff \rho \geq \frac{1-\alpha}{2m} = \rho_0.$$

Hence for $\rho \in [\rho_0, 1/m)$, the point $x^* = x_c^* e_c$ satisfies all KKT conditions. Since F_ρ is α -strongly convex, these KKT conditions certify that x^* is the unique minimizer and $S^* = \{c\}$. Finally, for any leaf ℓ (with $d_\ell = 1$) the degree-normalized slack is

$$\gamma_\ell = \frac{\lambda_\ell - |\nabla_\ell f(x^*)|}{\sqrt{d_\ell}} = \alpha\rho - \frac{1-\alpha}{2\sqrt{m}}x_c^* = \alpha\rho - \frac{1-\alpha}{2\sqrt{m}} \cdot \frac{2\alpha(1-\rho m)}{(1+\alpha)\sqrt{m}} = \frac{2\alpha}{1+\alpha}(\rho - \rho_0),$$

so at $\rho = \rho_0$ we indeed have $\gamma = 0$. ■

C.2 Path graph (seed at an endpoint)

Let $G = P_{m+1}$ be the path on nodes $1, 2, \dots, m+1$ with edges $(i, i+1)$. Let $s = e_1$ (seed at endpoint 1). Assume $m \geq 2$, so that $d_1 = d_{m+1} = 1$ and $d_i = 2$ for $2 \leq i \leq m$. Consider candidates of the form $x = x_1 e_1$.

Lemma C.2 (Path graph breakpoint: γ can be 0) Fix $\alpha \in (0, 1]$ and $m \geq 2$ and define

$$\rho_0 := \frac{1-\alpha}{3+\alpha}.$$

For any $\rho \in [\rho_0, 1)$, the unique minimizer has support $S^* = \{1\}$, with

$$x_1^* = \frac{2\alpha(1-\rho)}{1+\alpha}.$$

Moreover, the degree-normalized KKT slack at node 2 (where $d_2 = 2$), with $\lambda_2 = \alpha\rho\sqrt{d_2} = \alpha\rho\sqrt{2}$, equals

$$\gamma_2 := \frac{\lambda_2 - |\nabla_2 f(x^*)|}{\sqrt{d_2}} = \frac{\alpha(3+\alpha)}{2(1+\alpha)}(\rho - \rho_0).$$

In particular, at the breakpoint $\rho = \rho_0$ one has $\gamma = 0$.

Proof Recall that $f(x) = \frac{1}{2}x^\top Qx - \alpha\langle D^{-1/2}s, x \rangle$, hence

$$\nabla f(x) = Qx - \alpha D^{-1/2}s, \quad Q = \frac{1+\alpha}{2}I - \frac{1-\alpha}{2}D^{-1/2}AD^{-1/2}.$$

Since $s = e_1$ and $d_1 = 1$, we have $D^{-1/2}s = e_1$. Also, for the edge $(1, 2)$ we have $(D^{-1/2}AD^{-1/2})_{21} = 1/\sqrt{d_2d_1} = 1/\sqrt{2}$, so

$$Q_{11} = \frac{1+\alpha}{2}, \quad Q_{21} = Q_{12} = -\frac{1-\alpha}{2\sqrt{2}}.$$

Assume $x^* = x_1^*e_1$ with $x_1^* > 0$. For the ℓ_1 -regularized PageRank objective $F_\rho(x) = f(x) + \alpha\rho\|D^{1/2}x\|_1 + \mathbb{I}_{\mathbb{R}_{\geq 0}}(x)$, the active KKT condition at node 1 is

$$\nabla_1 f(x^*) = -\alpha\rho\sqrt{d_1} = -\alpha\rho.$$

But $\nabla_1 f(x^*) = (Qx^*)_1 - \alpha = Q_{11}x_1^* - \alpha$, hence

$$0 = \nabla_1 f(x^*) + \alpha\rho = Q_{11}x_1^* - \alpha + \alpha\rho = \frac{1+\alpha}{2}x_1^* - \alpha + \alpha\rho,$$

which yields

$$x_1^* = \frac{2\alpha(1-\rho)}{1+\alpha},$$

and this is positive iff $\rho < 1$. Now consider node 2 (which is inactive under our candidate). Since $(D^{-1/2}s)_2 = 0$ and x^* is supported only on node 1,

$$\nabla_2 f(x^*) = (Qx^*)_2 = Q_{21}x_1^* = -\frac{1-\alpha}{2\sqrt{2}}x_1^* \leq 0,$$

so

$$|\nabla_2 f(x^*)| = \frac{1-\alpha}{2\sqrt{2}}x_1^*.$$

The inactive KKT condition at node 2 requires $|\nabla_2 f(x^*)| \leq \alpha\rho\sqrt{d_2} = \alpha\rho\sqrt{2}$. Substituting x_1^* gives

$$\frac{1-\alpha}{2\sqrt{2}} \cdot \frac{2\alpha(1-\rho)}{1+\alpha} \leq \alpha\rho\sqrt{2} \iff \frac{(1-\alpha)(1-\rho)}{1+\alpha} \leq 2\rho \iff \rho \geq \frac{1-\alpha}{3+\alpha} = \rho_0.$$

For nodes $i \geq 3$, we have $(Qx^*)_i = Q_{i1}x_1^* = 0$ because node 1 is adjacent only to node 2, and also $(D^{-1/2}s)_i = 0$, hence $\nabla_i f(x^*) = 0$, which satisfies the inactive KKT interval $[-\alpha\rho\sqrt{d_i}, 0]$. Therefore, for any $\rho \in [\rho_0, 1)$, the point $x^* = x_1^*e_1$ satisfies all KKT conditions. Since F_ρ is α -strongly convex, this certifies that x^* is the unique minimizer and $S^* = \{1\}$.

Finally, the degree-normalized slack at node 2 is

$$\begin{aligned} \gamma_2 &= \frac{\lambda_2 - |\nabla_2 f(x^*)|}{\sqrt{d_2}} = \frac{\alpha\rho\sqrt{2} - \frac{1-\alpha}{2\sqrt{2}}x_1^*}{\sqrt{2}} = \alpha\rho - \frac{1-\alpha}{4}x_1^* \\ &= \alpha\rho - \frac{1-\alpha}{4} \cdot \frac{2\alpha(1-\rho)}{1+\alpha} = \frac{\alpha}{2(1+\alpha)} \left((3+\alpha)\rho - (1-\alpha) \right) = \frac{\alpha(3+\alpha)}{2(1+\alpha)} (\rho - \rho_0), \end{aligned}$$

and at $\rho = \rho_0$ this slack is 0, so $\gamma = 0$. ■

D Experimental setting details

This section collects the common experimental ingredients used throughout the synthetic experiments in [Sections 5.1](#) and [5.2](#). All experiments solve the ℓ_1 -regularized PageRank objective (RPPR) and report runtime using the degree-weighted work metric in [\(3\)](#). When we refer to the no-percolation diagnostic, we mean the inequality from [Theorem 4.4](#).

Synthetic graph family: core-boundary-exterior construction. Each synthetic instance is an undirected graph with a three-way partition of the node set $V = S \cup \mathcal{B} \cup \text{Ext}$, where S is a core (containing the seed), \mathcal{B} is a boundary region, and Ext is an exterior. The construction is deterministic. Given sizes $|S|$, $|\mathcal{B}|$, and $|\text{Ext}|$, edges are added according to the following rules:

- *Core clique.* The induced subgraph on S is a complete graph (a clique).
- *Core-boundary connectivity.* Let the core nodes be ordered as $S = \{0, 1, \dots, |S| - 1\}$ and let the boundary nodes be stored in an ordered list $(b_0, b_1, \dots, b_{|\mathcal{B}|-1})$. Each core node has c_{bnd} boundary per core neighbors in \mathcal{B} . For each core node $u \in S$ and each $j \in \{0, 1, \dots, c_{\text{bnd}} - 1\}$ we add the edge $(u, b_{(u \cdot c_{\text{bnd}} + j) \bmod |\mathcal{B}|})$. When $|\mathcal{B}| \geq c_{\text{bnd}}$ (as in our sweeps), this gives c_{bnd} distinct boundary neighbors per core node. Each core node has fixed degree $d_u = (|S| - 1) + c_{\text{bnd}}$ for $|\mathcal{B}| > 0$.
- *Boundary internal connectivity.* The boundary induces a circulant graph with an even degree parameter $\deg_{\mathcal{B}}$, capped at $|\mathcal{B}| - 1$, and adjusted to be even.
- *Exterior internal connectivity.* The exterior induces a circulant graph with degree \deg_{Ext} , with $\deg_{\text{Ext}} < |\text{Ext}|$.
- *Boundary-exterior connectivity.* Each exterior node has exactly one neighbor in \mathcal{B} , using the same rule as above, so the number of boundary-exterior edges equals $|\text{Ext}|$.

This construction yields a dense core, an internally connected boundary band, and a highly connected exterior, with sparse cross-region interfaces. When we visualize adjacency matrices, this produces a clear block structure (core | boundary | exterior) and a boundary region whose size/volume can be varied independently of the core neighborhood.

Optimization objective and parameters. On each graph instance we solve the ℓ_1 -regularized PageRank objective (RPPR) with a single-node seed $s = e_v$. Unless otherwise specified, the seed node v is a fixed core vertex (in the code, $v = 0$). Each experiment specifies a teleportation parameter $\alpha \in (0, 1]$ and a sparsity parameter $\rho > 0$. When using FISTA we set the momentum parameter to the standard strongly-convex choice $\beta := \frac{1 - \sqrt{\alpha}}{1 + \sqrt{\alpha}}$ (for PageRank, $L = 1$ and $\mu = \alpha$). Both ISTA and FISTA are initialized at $x_{-1} = x_0 = 0$.

Stopping criterion. All experiments compare ISTA and FISTA under the same KKT surrogate based on the proximal-gradient fixed point. With unit step size, define the prox-gradient map

$$T_{\alpha, \rho}(x) := \text{prox}_g(x - \nabla f(x)), \quad r(x) := \|x - T_{\alpha, \rho}(x)\|_{\infty}.$$

A point x^* is optimal for (RPPR) if and only if $x^* = T_{\alpha, \rho}(x^*)$, i.e., $r(x^*) = 0$. We therefore declare convergence when the fixed-point residual satisfies $r(x_k) \leq \varepsilon$, where $\varepsilon > 0$ is the prescribed tolerance. This termination rule is applied identically to ISTA and FISTA. In the work-vs- ε sweeps, the x -axis parameter is this residual tolerance ε ; for the other sweeps, ε is held fixed (and we impose a single large global iteration cap, e.g. 50,000, for all runs).

Degree-weighted work model. We measure runtime via a degree-weighted work model (3). For an iterate pair (y_k, x_{k+1}) we define the per-iteration work as $\text{work}_k := \text{vol}(\text{supp}(y_k)) + \text{vol}(\text{supp}(x_{k+1}))$. For ISTA, $y_k = x_k$; for FISTA, $y_k = x_k + \beta(x_k - x_{k-1})$. The work to reach the stopping target is the sum of work_k over the iterations taken.

No-percolation diagnostic. The no-percolation assumption (7) is satisfied for all our synthetic experiments. Conceptually, this condition is favorable for accelerated methods: it rules out “percolation” of extrapolated iterates into the exterior, so FISTA is not penalized by activating a large, highly connected ambient region. Nevertheless, our sweeps still exhibit regimes where FISTA does not improve work (and can be slower than ISTA), showing that even when exterior exploration is provably suppressed, acceleration can lose due to transient boundary activations.

Default synthetic parameters. Unless a sweep varies them, the synthetic experiments use the baseline block sizes and degrees $|S| = 60$, $|\text{Ext}| = 1000$, $c_{\text{bnd}} = 20$, $\deg_{\mathcal{B}} = 82$, $\deg_{\text{Ext}} = 998$, and a fixed seed $v \in S$ (node 0 in the implementation). The specific sweep parameter(s) are described in the corresponding experiment sections.

Per-point graph generation and how to read sweep plots. Our theory gives instance-wise guarantees (each bound applies to every graph in the family), and the synthetic family itself is specified by coarse structural parameters (block sizes and target degrees), not a single fixed adjacency matrix. Accordingly, in several sweeps we intentionally regenerate the synthetic instance at each x -axis value. In these cases, each dot should be interpreted as one representative draw from the family at that parameter value, i.e., a snapshot of what can happen empirically under the same coarse structure. This design avoids conclusions that are artifacts of one particular synthetic realization and is aligned with the worst-case nature of the theory.

E Full details for the fixed-boundary sweeps experiments

We provide full details for the experiments in Section 5.2. We follow the synthetic construction, algorithmic choices, and work-metric conventions from Section D, and fix the boundary size to $|\mathcal{B}| = 600$. We sweep ρ (with fresh graphs

per point), and we additionally sweep α and the fixed-point residual tolerance ε with $\rho = 10^{-4}$ fixed (and all other baseline parameters fixed).

This experiment complements the boundary-volume sweep of [Section 5.1](#) by holding the boundary size fixed ($|\mathcal{B}| = 600$) and varying only the regularization strength ρ . The aim is to isolate the ρ -dependence suggested by [Theorem 4.3](#) (both terms scale as $1/\rho$ when α and the boundary are fixed), and to check whether ISTA and FISTA respond similarly as ρ increases, since their worst-case theoretical running time depends on ρ in the same way. We run two versions of the ρ -sweep, both using a randomized graph per ρ :

- *Dense-core sweep.* The core subgraph is a clique, see [Section D](#).
- *Sparse-core sweep.* The core subgraph is sparsified by retaining a fixed fraction of its edges while enforcing that the core remains connected (implemented by sampling a random spanning tree and then adding random core-core edges up to the target density). In the sparse variant used here we keep 20% of the clique edges. We perform experiments on the sparsified-core variant to verify that the observed ρ -dependence is not an artifact of the highly symmetric clique core: sparsifying reduces and heterogenizes core/seed degrees. For both variants, we sweep ρ over a log-spaced grid chosen so that the no-percolation inequality holds for all sampled values.

The next experiment sweeps α , while keeping all other parameters fixed. Sweeping α to smaller values makes the no-percolation condition more stringent. Rather than reweighting edges, we keep the graph unweighted and use an α -sweep-specific graph family in which the exterior is a complete graph on $|\text{Ext}|$ nodes, and only a prescribed number m of exterior nodes have a single boundary neighbor (the remaining exterior nodes have no boundary neighbor). We choose $|\text{Ext}|$ so that the no-percolation inequality holds at the smallest swept value α_{\min} ; since the left-hand side decreases with α , this implies no-percolation for all $\alpha \geq \alpha_{\min}$ in the sweep.

The α sweep in our code additionally includes an auto-tuning step that selects a single unweighted instance from this family before running the sweep. Concretely, the tuner searches over: (i) the core-boundary fanout c_{bnd} (boundary neighbors per core node), (ii) the boundary internal circulant degree, and (iii) the number m of exterior-to-boundary edges (one boundary neighbor for each of the first m exterior nodes), with $|\text{Ext}|$ set to the smallest value that enforces no-percolation at α_{\min} . For each candidate, it evaluates performance on a calibration grid of 12 log-spaced α values in $[\alpha_{\min}, 0.9]$ and chooses the candidate that maximizes the fraction of calibration points where FISTA incurs larger work than ISTA. This is meant to illustrate that acceleration can be counterproductive on some valid instances even when iteration complexity improves.

For the ε sweep, we keep $\alpha = 0.20$ fixed and vary the fixed-point residual tolerance over a log-spaced grid $\varepsilon \in [10^{-12}, 10^{-1}]$. We use the original baseline instance (no auto-tuning and no graph modification).

F Additional real-data diagnostics

In this section we interpret the results of the experiments on real data from [Section 5.3](#).

Diagnosing slowdowns: iterations vs. per-iteration work. The work metric counts degree-weighted support volumes touched by both the extrapolated point y_k and the proximal update, so FISTA can lose either by taking more iterations than ISTA or by having a larger per-iteration locality cost. To separate these effects, for each seed (at $\alpha = 10^{-3}$, $\rho = 10^{-4}$, $\varepsilon = 10^{-8}$) we plot

$$\text{iteration ratio} = \frac{N_{\text{F}}}{N_{\text{I}}} \quad \text{vs.} \quad \text{per-iter ratio} = \frac{(W_{\text{F}}/N_{\text{F}})}{(W_{\text{I}}/N_{\text{I}})},$$

where $N_{\text{I}}, N_{\text{F}}$ are iteration counts and $W_{\text{I}}, W_{\text{F}}$ are total works. Since $\frac{W_{\text{F}}}{W_{\text{I}}} = \frac{N_{\text{F}}}{N_{\text{I}}} \cdot \frac{(W_{\text{F}}/N_{\text{F}})}{(W_{\text{I}}/N_{\text{I}})}$, points with both ratios above 1 correspond to clear slowdowns. [Figure 7](#) shows that on `com-Orkut` at $\alpha = 10^{-3}$, FISTA is frequently slower because it often incurs both a larger iteration count and a larger per-iteration work cost, whereas on the other datasets FISTA typically reduces iterations while paying a moderate per-iteration locality overhead.

Degree heterogeneity. Because our work metric is degree-weighted, transient activations of even a small number of high-degree nodes can dominate the locality cost. [Figure 8](#) plots the empirical degree complementary CDF for the four datasets and highlights the substantially heavier tail of `com-Orkut` (and, to a lesser extent, `com-Youtube`), which is consistent with the larger variability and the small- α slowdowns observed in [Figures 4](#) and [7](#).

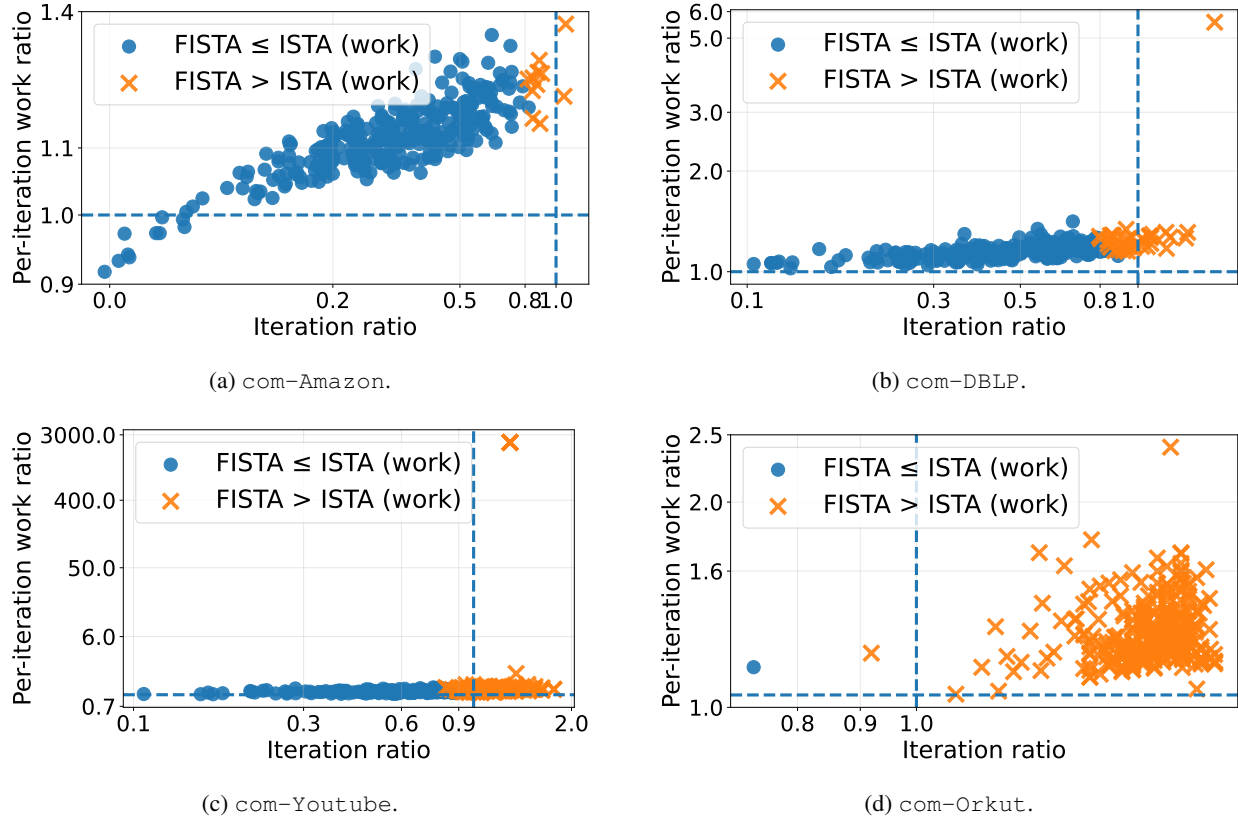


Figure 7: *Iterations vs. per-iteration work tradeoff*. Each point is a seed node (same seeds as in the sweep experiments), at $\alpha = 10^{-3}$, $\rho = 10^{-4}$, and $\varepsilon = 10^{-8}$. The x -axis is the iteration ratio N_F/N_I and the y -axis is the per-iteration work ratio $(W_F/N_F)/(W_I/N_I)$. Markers distinguish seeds where FISTA is faster/slower in total work.

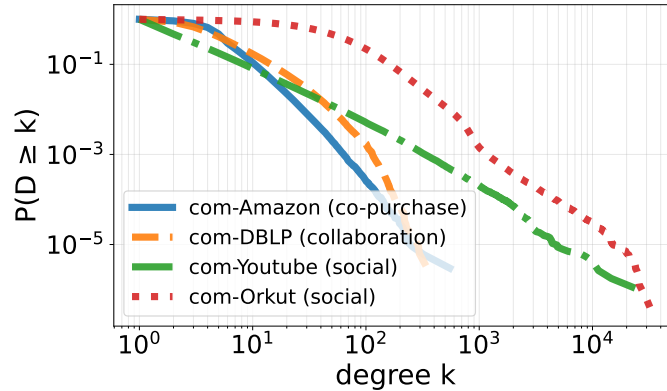


Figure 8: *Degree distributions on the real datasets*. The heavier-tailed degree profiles (notably `com-Orkut`) amplify the impact of transient exploration.

G AI-assisted development and prompt traceability

This paper was developed with the assistance of an interactive large-language-model (LLM) workflow. The LLM was used as a proof-synthesis and rewriting aid: it generated candidate lemmas, algebraic manipulations, and \LaTeX skeletons, while the human author(s) provided the research direction, imposed algorithmic constraints, requested specific locality-aware bounds, identified missing assumptions, and validated (or rejected) intermediate arguments. The

final statements and proofs appearing in the paper were human-checked and edited for correctness and presentation.

G.1 Prompt clusters and how they map to results in the paper

The interactive prompting that led to the final results naturally grouped into a small number of “prompt clusters.” Below we summarize each cluster, the key human supervision intervention(s), and the resulting manuscript artifacts (with cross-references). We use GPT-5.2 Pro (extended thinking) for all results and experiments.

(P1) “Standard accelerated algorithm only; avoid expensive subproblems.” The initial constraint was to analyze classic one-gradient-per-iteration acceleration (FISTA) rather than outer-inner schemes or methods that solve expensive auxiliary subproblems. This constraint fixed the algorithmic object of study and ruled out approaches akin to expanding-subspace or repeated restricted solves. It directly shaped the scope of the main runtime result [Theorem 4.3](#) and the fact that all bounds are expressed in the degree-weighted work model.

(P2) “Use the margin/KKT slack idea.” This idea was suggested by GPT, but we found it useful and, therefore, retained it in the final results. A key prompt requested a self-contained argument based on a margin parameter. This produced the degree-normalized slack definition [\(5\)](#) and its operational meaning: an inactive coordinate can become active at an extrapolated point only if its forward-gradient map deviates from the optimum by an amount proportional to its slack. The corresponding quantitative statement is [Lemma 4.1](#), which is the main bridge from optimality structure to spurious activations.

(P3) “Transient support is the bottleneck; bound the sum of supports/volumes.” A crucial human intervention was to point out that it is not enough to argue eventual identification: one must control the cumulative degree-weighted work over the entire transient. This prompted the transition from pointwise identification to a global summation argument: Cauchy-Schwarz converts “activation implies a jump” (from [Lemma 4.1](#)) into a bound on $\sum_k \text{vol}(A_k)$, and geometric contraction of FISTA controls the resulting series. This is the backbone of the spurious-work bound in the proof of [Theorem 4.3](#) (see in particular the derivation around [\(8\)](#)).

(P4) “Avoid vacuous bounds when the minimum margin is tiny; use over-regularization.” Another human-directed prompt asked how to proceed when the minimum slack can be arbitrarily small, which would make any bound that depends on $\min_{i \in I^*} \gamma_i$ meaningless. Thus the idea for analyzing a more regularized problem (“(B)”) but treating nearly-active nodes as part of the target support of the less-regularized problem (“(A)”) was suggested to the LLM. Concretely, this yielded the split in [Lemma 4.2](#), which uses regularization-path monotonicity (cf. [Lemma A.4](#)) to show that “small (B)-margin” nodes must lie in S_A and should not be charged as spurious. This is a key input to the work bound [Theorem 4.3](#).

(P5) “Turn the work bound into a running-time bound using $\text{vol}(S^*) \leq 1/\rho$.” A prompt explicitly requested that the final complexity be stated in the degree-weighted work model and use the known sparsity guarantee $\text{vol}(S^*) \leq 1/\rho$. This guided the decomposition [\(4\)](#) into “work on the target support” plus “spurious work,” and it is the reason the first term in [Theorem 4.3](#) scales as $\tilde{O}((\rho\sqrt{\alpha})^{-1})$ (up to logarithms).

(P6) “Give a checkable confinement condition so spurious activations stay local.” After the spurious-work summation bound was obtained, a prompt requested a graph-checkable assumption guaranteeing that all spurious activations remain confined to a boundary set. This produced the exposure/no-percolation-style sufficient condition formalized as [Theorem 4.4](#), which is referenced immediately after [Theorem 4.3](#) to justify the boundary-set hypothesis $\hat{A}_k \subseteq \mathcal{B}$.

(P7) “Identify explicit bad instances where γ can be very small (or 0).” To stress-test the margin-based reasoning, a sequence of prompts asked for explicit graphs where the slack is smaller than $\sqrt{\rho}$ and even $o(\sqrt{\rho})$. This led to the breakpoint constructions recorded in [Section C](#), including the star graph ([Lemma C.1](#)) and the path graph ([Lemma C.2](#)). These examples motivate why the paper avoids global dependence on γ and instead relies on the over-regularization/two-tier strategy ([Lemma 4.2](#)) together with confinement ([Theorem 4.4](#)).

(P8) “High-degree non-activation under over-regularization.” A later prompt suggested to use the overregularization idea to rule out spurious activations of very high-degree nodes. This yielded the explicit degree cutoff condition in [Proposition B.1](#), which provides an additional structural non-activation guarantee that complements the boundary-confinement approach.

(P9) “Experiments.” All code was generated by the LLM. However, the authors heavily supervised the process.

G.2 How much human supervision was required?

The development required human-in-the-loop supervision. Across roughly two dozen interactive turns, the human prompts performed tasks that the LLM did not do reliably on its own:

- **Problem framing and constraints.** The human author fixed the algorithmic scope (standard FISTA; no expensive subproblems) and demanded a locality-aware work bound rather than a standard iteration bound (driving [Theorem 4.3](#)).
- **Identifying the real bottleneck.** A key correction was the insistence that bounding eventual identification is insufficient; one must bound the sum of transient supports/volumes (leading to the summation argument in the proof of [Theorem 4.3](#)).
- **Stress-testing with counterexamples.** The human prompts requested explicit worst cases (star and path) and used them to diagnose when naive γ -based bounds become vacuous (motivating [Section C](#) and the over-regularization strategy used in [Lemma 4.2](#)).
- **Assumption checking and proof repair.** When an intermediate proof relied on an unproven positivity/sign assumption, the human author demanded either a proof or a repair; this resulted in a revised subgradient/KKT-based certificate (ultimately not needed for the core theorems, but an important correctness checkpoint).
- **\LaTeX integration/debugging.** Compile errors and presentation issues (e.g., list/itemization mistakes) were identified via human compilation and corrected in subsequent iterations.

Overall, the LLM contributed most effectively as a rapid generator of candidate proofs and algebraic manipulations, while the human supervision was essential for (i) setting the right target statement, (ii) insisting on the correct work metric, (iii) enforcing locality constraints, (iv) catching missing assumptions, and (v) selecting which generated material belonged in the final paper.